

Attachment 1

Benoni B., Potužník J. F., Škríba A., Benoni R., Trylcova J., Tulpa M., Spustová K., Grab K., Mititelu M.B., Pačes J., Weber J., Stanek D., Kowalska J., Bednarova L., Keckesova Z., Vopalensky P., Gahurova L. and Cahova H. "HIV-1 infection reduces NAD capping of host cell snRNA and snoRNA". *ACS Chemical Biology* 2024 19 (6), 1243-1249.

IF(2024) = 3.5

Attachment 2

Šimonová A., **Svojanovská B.**, Trylčová J., Hubálek M., Moravčík O., Zavřel M., Pávová M., Hodek J., Weber J., Cvačka J., Pačes J., Cahová H. "LC/MS analysis and deep sequencing reveal the accurate RNA composition in the HIV-1 virion." *Scientific Reports* 2019 9(1): 8697.

IF(2019) = 3.99

Attachment 3

Šimonová A., Romanská V., **Benoni B.**, Škubník K., Šmerdová L., Procházková M., Spustová K., Moravčík O., Gahurova L., Pačes J., Plevka P., Cahová H. "Honeybee Iflaviruses Pack Specific tRNA Fragments from Host Cells in Their Virions." *ChemBioChem* 2022 23(17): e202200281.

IF(2022) = 3.2

HIV-1 Infection Reduces NAD Capping of Host Cell snRNA and snoRNA

Barbora Benoni, Jiří František Potužník, Anton Škríba, Roberto Benoni, Jana Trylcova, Matouš Tulpa, Kristína Spustová, Katarzyna Grab, Maria-Bianca Mititelu, Jan Pačes, Jan Weber, David Stanek, Joanna Kowalska, Lucie Bednarova, Zuzana Keckesova, Pavel Vopalensky, Lenka Gahurova, and Hana Cahova*



Cite This: *ACS Chem. Biol.* 2024, 19, 1243–1249



Read Online

ACCESS |



Metrics & More

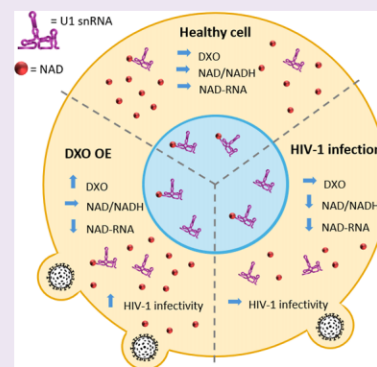


Article Recommendations



Supporting Information

ABSTRACT: Nicotinamide adenine dinucleotide (NAD) is a critical component of the cellular metabolism and also serves as an alternative 5' cap on various RNAs. However, the function of the NAD RNA cap is still under investigation. We studied NAD capping of RNAs in HIV-1-infected cells because HIV-1 is responsible for the depletion of the NAD/NADH cellular pool and causing intracellular pellagra. By applying the NAD captureSeq protocol to HIV-1-infected and uninfected cells, we revealed that four snRNAs (e.g., U1) and four snoRNAs lost their NAD cap when infected with HIV-1. Here, we provide evidence that the presence of the NAD cap decreases the stability of the U1/HIV-1 pre-mRNA duplex. Additionally, we demonstrate that reducing the quantity of NAD-capped RNA by overexpressing the NAD RNA decapping enzyme DXO results in an increase in HIV-1 infectivity. This suggests that NAD capping is unfavorable for HIV-1 and plays a role in its infectivity.



To date, more than 170 RNA modifications have been discovered.¹ Among the least explored RNA modifications are 5' noncanonical RNA caps, including nicotinamide adenine dinucleotide (NAD),² flavin adenine dinucleotide,³ and dinucleoside polyphosphates.^{4,5} Because they are typically detected through LC–MS analysis of digested RNA, there is no information on which RNA sequences bear these caps. Several methods have been developed for the sequencing of NAD–RNA. The original NAD captureSeq protocol^{6,7} was later modified, resulting in various protocols such as SPAAC–NAD–Seq,⁸ or NADcapPro, circNC,⁹ and ONE–seq.¹⁰ These methods allow for the identification of NAD–RNA sequences in various organisms (e.g., *Staphylococcus aureus*,¹¹ *Saccharomyces cerevisiae*,¹² and human cells¹³). NAD has been detected as a 5' RNA cap attached to small regulatory RNAs in bacteria⁶ and various mRNAs in higher organisms.¹⁴ Recently, NAD–RNA was also reported to function as a substrate for the RNylation of proteins upon phage infection in bacteria.¹⁵ However, the role of this cap in higher organisms remains unclear.

Because HIV-1 infection of human cells depletes the cellular pool of free NAD,¹⁶ we envisaged it as a physiologically interesting model system in which to study the role of the NAD RNA cap. There are two different mechanisms responsible for NAD depletion. First, there is an increased activity of CD38 in HIV-1-infected cells, which reduces the NAD pool.¹⁷ The second mechanism includes the activation of poly(ADP–ribose) polymerases (PARPs), induced by oxida-

tive stress during HIV-1 infection,^{18,19} which consume NAD and thus trigger de novo niacin synthesis (precursor of NAD). Moreover, it has been reported that nicotinamide acts as an inhibitor of HIV-1 infection.²⁰ For this reason, niacin has been suggested as a potential AIDS preventive factor.²¹ In addition, the genetic variation in the locus of the NAD decapping enzyme DXO is associated with differences in the response to HIV-1 infection.²²

Here, we report that subsets of cellular snRNAs and snoRNAs lose the NAD cap after HIV-1 infection. Among these RNAs we detected U1 snRNA, which is essential for viral replication.^{23,24} We found that, in comparison with 7,7,2-trimethylguanosine (TMG)-capped U1 snRNA,²⁵ the NAD cap has a destabilizing effect on the binding of U1 snRNA to viral pre-mRNA. This suggests that the NAD RNA cap reduces the binding of U1 snRNA with the viral RNA target and might thus contribute to the protection against HIV-1 infection. To test this hypothesis, we overexpressed and knocked down the NAD decapping enzyme DXO and monitored HIV-1 production. The overexpression of DXO, which decreases

Received: March 1, 2024

Revised: May 9, 2024

Accepted: May 10, 2024

Published: May 15, 2024



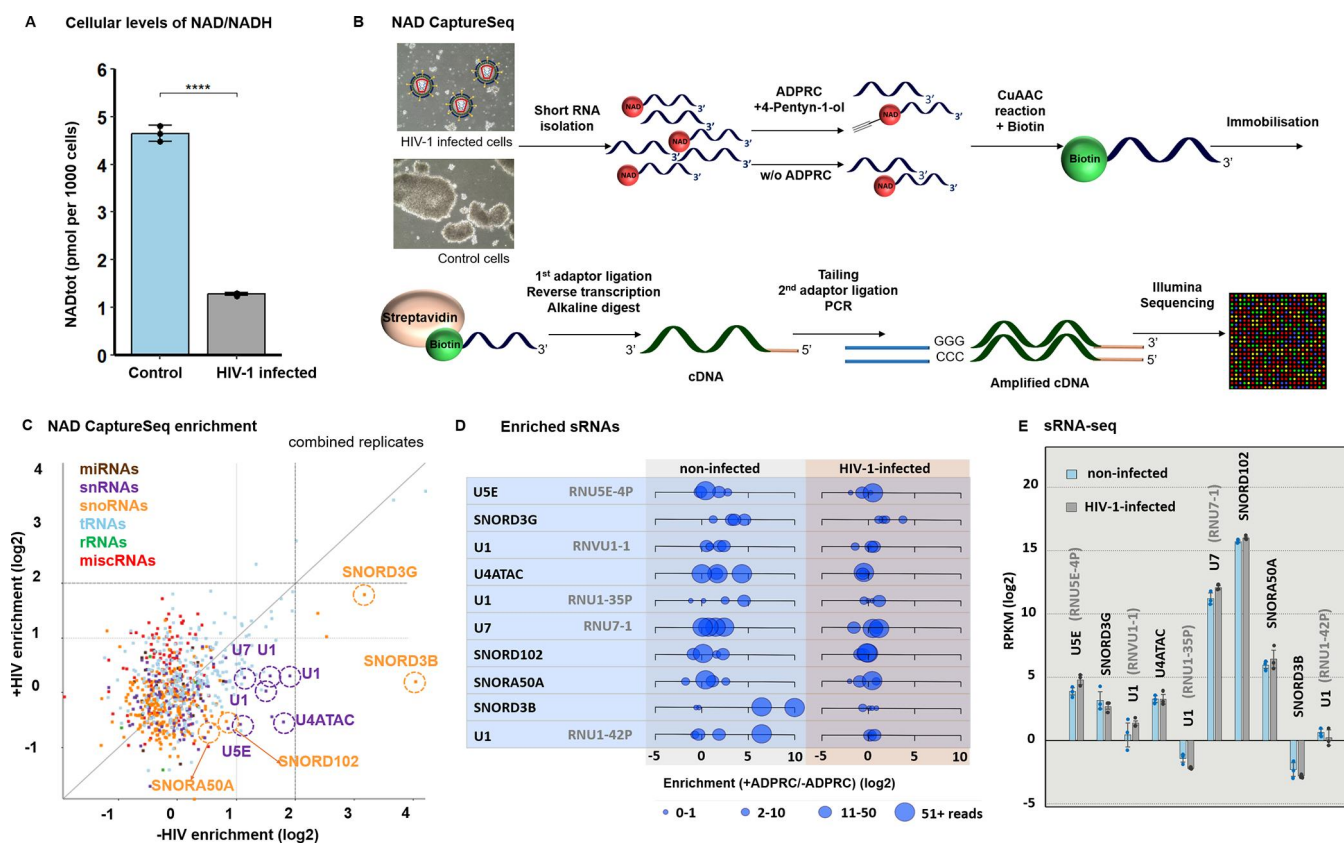


Figure 1. Changes in NAD RNA capping upon HIV-1 infection. (A) Levels of free NAD/NADH in control and HIV-1-infected cells (measured in biological triplicates and technical duplicates, *t*-test). (B) Scheme of the NAD captureSeq protocol applied to control and HIV-1-infected cells. (C) Scatter plot showing the NAD captureSeq enrichment (+ADPRC vs −ADPRC) in control (*X*-axis) and HIV-1-infected samples (*Y*-axis), showing average values across replicates. Highlighted sRNAs passed the criteria listed in Figure S1B, i.e., change in NAD cap abundance upon HIV-1 infection, having specific enrichment in +ADPRC samples, sufficient read count and consistency across replicates; these sRNAs are visualized in more detail for individual replicates in panel (D). (D) Enrichment of RNAs in NAD captureSeq analysis enriched in control cells versus HIV-1-infected cells, matching highlighted sRNAs in Figure 1C. Blue circles show individual replicates; the size of the circle corresponds to the number of mapped reads. (E) sRNA-seq analysis of identified candidate sRNAs in control and HIV-1-infected cells (prepared in biological triplicates).

cellular levels of NAD-capped RNAs, results in higher virus infectivity. These findings provide the first link between cellular NAD/NADH levels, NAD capping, and HIV-1 infectivity.

It has been reported that HIV-1 infection causes intracellular pellagra, meaning the depletion of the NAD/NADH pool in the cell;¹⁶ therefore, we measured the total concentration of NAD in control (uninfected) MT4 cells and MT4 cells infected with HIV-1 (Figure 1A). Indeed, we observed a nearly four times greater intracellular concentration of NAD in control cells, compared to infected cells. Because NAD is incorporated into RNA co-transcriptionally by RNA polymerases as a noncanonical initiating nucleotide,²⁶ we hypothesized that a change in the intracellular level of NAD may also influence the NAD capping of RNA.

As studies of the NAD cap in mRNA are yet to arrive at a clear-cut explanation of its role, we focused on the potential effect of the NAD RNA cap on short noncoding regulatory RNAs (sRNA). The fraction of sRNA usually contains various regulatory RNAs that bind to their targets and where RNA caps could affect the recognition and binding and, thus, it might be easier to study the functional role of the cap itself. Therefore, we investigated how HIV-1 infection affects the extent of NAD capping of sRNA. To identify RNAs with altered NAD capping, we prepared four NAD captureSeq

libraries from the sRNA fraction of control and HIV-1-infected cells. The NAD captureSeq protocol^{6,7} relies on a selective reaction of ADP-ribosyl cyclase (ADPRC) with 4-pentyn-1-ol and with NAD-RNA (see Figure 1B, as well as Table S1), which allows for the enrichment of previously NAD-capped RNA and subsequent RNaseq analysis. To sort out nonspecifically interacting RNA, ADPRC was omitted in negative control samples (−ADPRC). Even though the m⁷G cap has been reported to partially react with ADPRC,⁹ the sRNA fraction we used contained ~5 times less m⁷Gp₃Am (cap1) per molecule of RNA than the long RNA (lRNA) fraction (Figure S1A). Therefore, we did not deplete m⁷G-capped RNA from our sRNA.

The sequenced NAD captureSeq libraries were mapped to both the human genome and that of HIV-1 (Figure S1B). We detected the NAD cap in 94 cellular sRNAs (2 miRNAs, 6 miscellaneous RNAs, abbreviated to miscRNA, 62 tRNAs, 12 snoRNAs, 12 snRNAs). Consistent with previous observations,¹³ we also detected the NAD cap on the 5′-end fragments of some mRNAs but not on the 5′ end of viral mRNA fragments (Figure S1C), which was previously shown to contain the TMG or m⁷G cap.²⁷ Overall, we observed similar quantities of enriched and depleted NAD-capped sRNAs in both HIV-1-infected and control cells (Figure 1C). However, with 42 NAD-capped sRNAs, these quantities varied

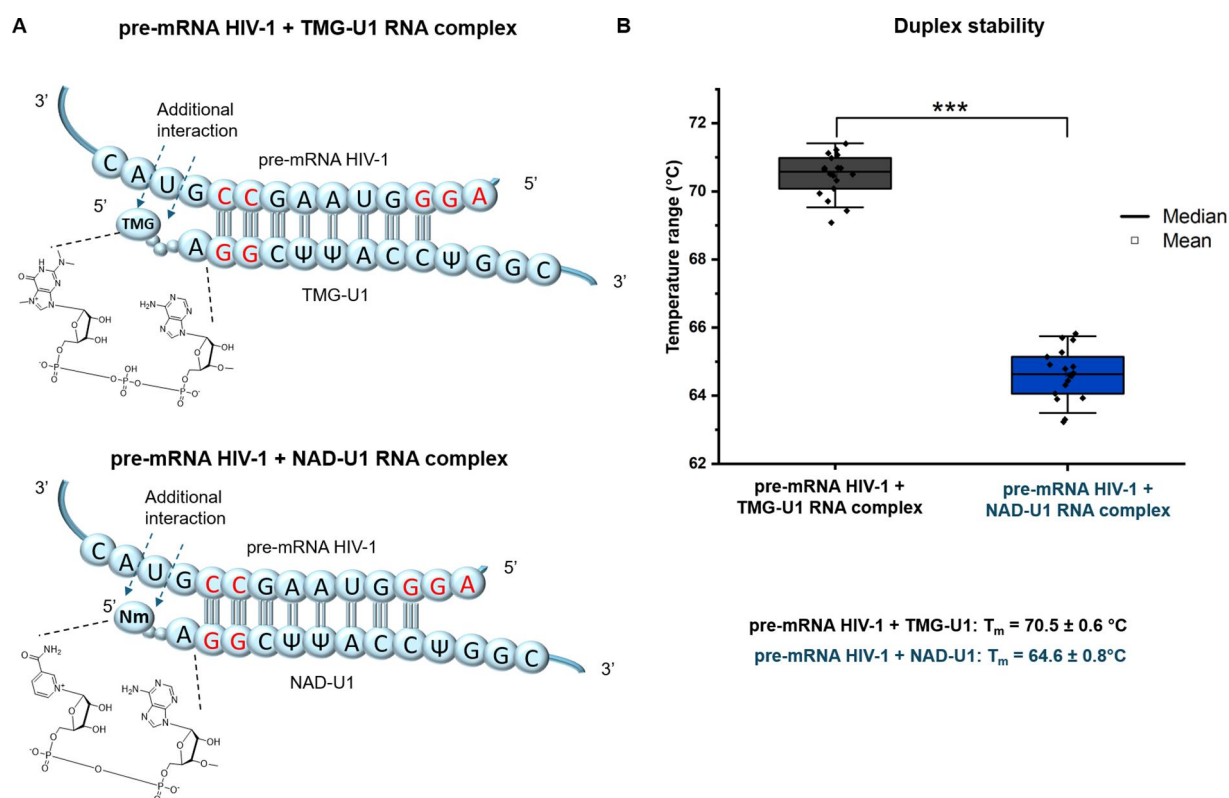


Figure 2. NAD cap of U1 snRNA destabilizes the complex with HIV-1 pre-mRNA. (A) Scheme of the complex formed by complementary regions of HIV-1 pre-mRNA with either TMG-U1 (top) or NAD-U1 (bottom). Nucleobase symbols in red mark positions mutated to meet the requirements of T7 RNA polymerase. (B) Duplex stability of HIV-1 pre-mRNA with TMG-U1 (dark gray) or NAD-U1 (blue) measured using a light cycler device (measured in triplicate in a series of nine measurements of each, *t*-test).

substantially between HIV-1-infected and control cells. An increase in NAD capping upon HIV-1 infection was detected on sRNAs known in the literature to be packed in HIV-1 virions (e.g., various tRNAs) (Figure S2);^{28,29} however, we did not pursue this observation further. Particularly prominent were hits with decreased NAD capping upon HIV-1 infection from two classes of sRNAs: snRNAs and snoRNAs. To filter out sRNAs that react nonspecifically in the +ADPRC reaction (measured by low enrichment in +ADPRC vs −ADPRC samples), we applied a set of criteria regarding the number of mapped reads and consistency across replicates (detailed parameters are listed in Figure S1B, sRNAs that passed each filtering step are given in Table S2). After this filtration, we identified four snoRNAs (SNORD3G, SNORD102, SNORA50A, and SNORD3B) and four snRNAs (U1, U4ATAC, USE, and U7) with decreased NAD capping upon HIV-1 infection (see Figures 1C and 1D).

Because the amount of total RNA in control and HIV-1-infected cells was similar (Figure S3A), we further investigated whether the decreased amount of the NAD-cap on particular sRNAs after HIV-1 infection is caused by altered sRNA expression. We prepared sRNA-seq libraries from control and infected cells and performed DESeq2 analysis. Out of the 2014 detected sRNAs (miRNAs, miscRNAs, tRNAs, snRNAs, snoRNAs, and rRNAs), 89 were identified as significantly differentially expressed: 52 sRNAs were upregulated and 37 downregulated after infection (Table S3 and Figures S3B and S3C). Neither of these 89 sRNAs was enriched in the NAD captureSeq protocol. Moreover, using these data, we confirmed that the expression levels of identified snRNA and snoRNA do not change after HIV-1 infection (Figure 1E). The sequencing

results were independently confirmed by RT-qPCR of selected sRNAs (Figure S4). These experiments exclude the possibility that changes in NAD-RNA enrichment in infected cells are caused by the differential expression of particular cellular RNAs upon HIV-1 infection.

Next, we also wanted to confirm the presence of the NAD cap in RNA from MT4 cells by means of LC-MS analysis. To avoid the detection of NAD noncovalently bound to RNA, we included a urea wash step³⁰ in our protocol. Isolated and washed RNA was treated with the NudC enzyme to cleave nicotinamide mononucleotide (NMN) from NAD-capped RNA. The NMN was then converted to nicotinamide riboside (NR) by employing shrimp alkaline phosphatase.³⁰ For the purposes of quantification, isotopically labeled (deuterated) D₃-NR was spiked in each sample as an internal standard. In general, we did not observe any statistical difference between infected and control cells in either sRNA or lRNA (Figures S5A–S5E). This observation might be explained by the fact that similar quantities of sRNAs are enriched or depleted in NAD captureSeq data in HIV-1-infected and control cells (Figure 1C). On the other hand, LC-MS analysis of U1 RNA pulled down from the sRNA fraction isolated from control and HIV-1-infected cells confirmed the significant depletion of the NAD cap on this particular RNA (Figures S6A–S6C). This finding shows that HIV-1 infection causes a decrease in the NAD capping of U1.

The U1 snRNA is known to play an important role in the lifecycle of HIV-1.^{24,31} The 5′ region (8 nucleotides) of U1 binds complementarily to the 5′ splice site of unspliced HIV-1 mRNA, which leads to the Rev-regulated translocation of partially spliced or unspliced HIV-1 mRNA into the cytosol.²³

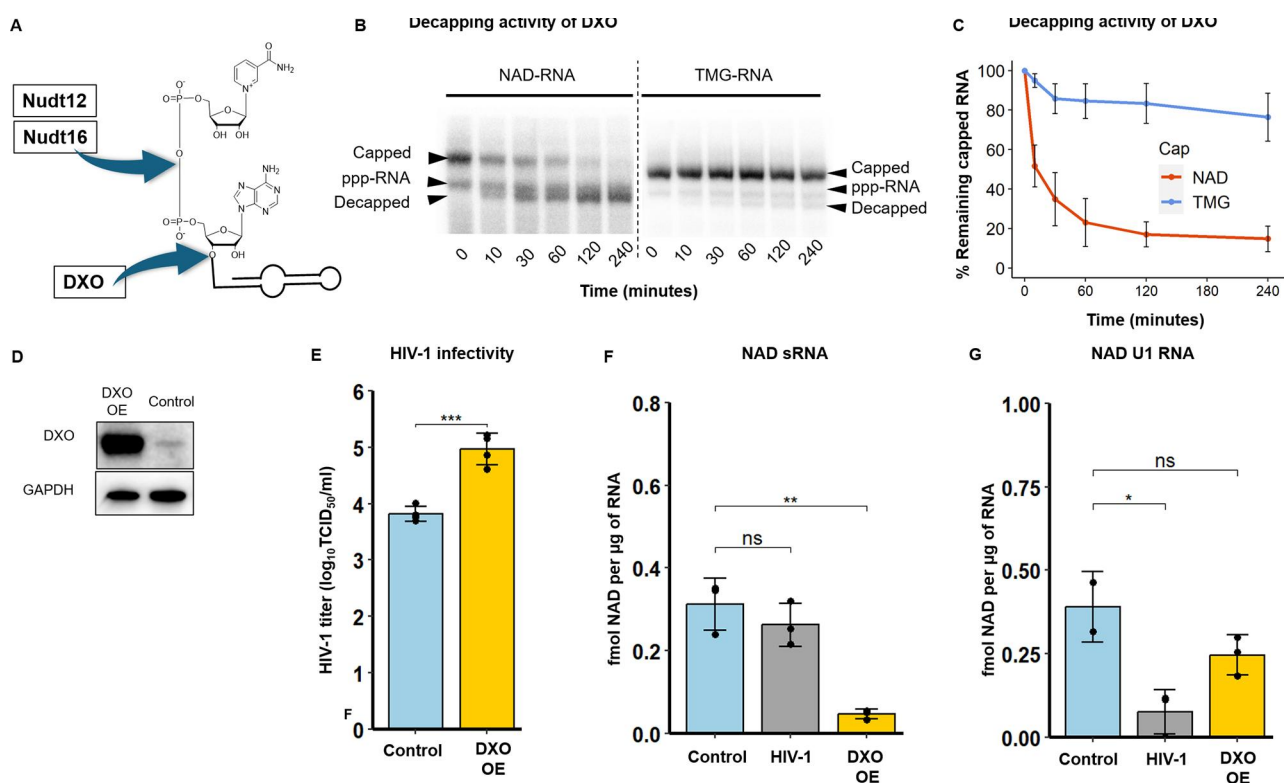


Figure 3. Decrease of NAD RNA capping leads to increased HIV-1 infectivity. (A) Cleavage positions of the NAD RNA cap by the three known decapping enzymes Nudt12, Nudt16 and DXO. (B) In vitro DXO cleavage of NAD-U1 and TMG-U1 at various time points (time (0, 10, 30, 60, 120 and 240 min)). (C) Quantification of DXO decapping activity based on PAGE gels (experiments performed in triplicate, error bar represents the standard deviation of the mean). (D) Western blot analysis of DXO and GAPDH (as a control) in control cells and cells with overexpressed (DXO OE). (E) HIV-1 infectivity determined in control cells and cells with overexpressed DXO (DXO OE) (ANOVA test). (F) LC-MS quantification of the NAD RNA cap level in sRNA isolated from control cells and cells with overexpressed DXO (DXO OE) (*t*-test). (G) LC-MS quantification of the NAD RNA cap level in pulled-down U1 RNA (*t*-test). All the experiments were performed at least in biological duplicates.

A single mutation in the 5' splice site of HIV-1 mRNA causes a significant decrease in HIV-1 replication due to limited binding of U1. This effect could be suppressed by co-transfection with U1 that restores base pairing with the mutated 5' splice site of HIV-1 pre-mRNA, which indicates the importance of U1/HIV-1 pre-mRNA base pairing.²³ We hypothesized that altered RNA capping of U1 (the 5' end that recognizes HIV-1 pre-mRNA) might influence the binding to pre-mRNA and its subsequent interaction with the Rev protein. This complex is then translocated to the cytosol and leads to the translation of envelope-encoding HIV-1 mRNA. In this way, the alteration of U1 capping might influence the viral replication cycle. For these reasons, we investigated the role of the 5' RNA cap of U1 in binding to HIV-1 pre-mRNA. Until now, it was assumed that U1 is naturally capped only with the TMG cap.²⁵ Here, we show that part of the cellular pool of U1 is also capped with NAD and that this cap gets depleted upon HIV-1 infection. We recently showed that some noncanonical RNA caps (e.g., Ap₃G) bind to DNA templates via noncanonical base pairing during transcription.³² Accordingly, we hypothesize that the NAD RNA cap may contribute to the binding of U1 to its target HIV-1 pre-mRNA and that it may negatively or positively influence the strength of the interaction. To test this hypothesis, we prepared 20-mer RNA mimicking the 5' U1 RNA region with either the NAD or the TMG cap (supplementary protocol) through in vitro transcription with T7 RNA polymerase (the original sequence AUA was changed to AGG due to the template requirements of T7 RNA

polymerase). Pseudo-uridine triphosphate (Ψ TTP) was used instead of UTP to mimic the natural presence of Ψ in positions 5 and 6 in U1 (Figure 2A). Furthermore, we prepared 20-mer RNA mimicking the D4 splice site of HIV-1 pre-mRNA complementary to U1. We measured the melting temperature (T_m) values of corresponding duplexes using an intercalating fluorophore and a light cyclor device. The T_m values of RNA duplexes in this assay were 70.5 ± 0.6 °C and 64.6 ± 0.8 °C for TMG-U1 and NAD-U1, respectively (Figure 2B). As in vitro transcription with Ψ TTP did not lead to a sufficient amount of RNA for circular dichroism (CD) spectroscopy studies, which are usually used for RNA duplex characterization, we prepared a 20-mer mimicking the 5' U1 RNA region with either the NAD or TMG cap without Ψ TTP (Figure S7A). The CD spectra of both duplexes with a positive maximum at 264 nm were typical for the right-handed A-type double helix of RNA (see Figures S7B and S7C) and confirmed the observation from the melting curve analysis on the light cyclor device (Figure S7D). The difference in the stability of duplexes with and without pseudo-uridine may be explained by a certain rigidity caused by the pseudo-uridines, which restricts the motion of neighboring nucleotides including the 5' cap.^{33,34} This experiment showed that the binding of TMG-U1 to HIV-1 pre-mRNA is much stronger than the NAD-U1 interaction with HIV-1 pre-mRNA. This indicates that the NAD cap reduces the binding of U1 to the target HIV-1 pre-mRNA sequence and thus may negatively influence HIV-1 replication.

The NAD cap is removed in human cells by these enzymes: Nudt12,³⁵ Nudt16,³⁶ and DXO.¹³ Nudt12 and Nudt16 members of the NudIX family, cleave the pyrophosphate backbone of free NAD³⁷ and NAD–RNA, and, thus, reduce the intracellular concentrations of free NAD and NAD–RNA, whereas DXO cleaves the entire moiety of NAD from RNA and does not affect the intracellular concentration of free NAD (Figure 3A).¹³ To investigate solely the role of NAD–RNA (not free NAD) in HIV-1 infection, we focused on the DXO decapping enzyme. In the following experiments, we wanted to explore the direct effect of changed NAD–RNA capping on HIV-1 infection and to distinguish it from the effect of the changed total NAD pool. Although it has been reported that DXO may cleave the TMG cap,³⁸ we show that NAD–RNA is its preferred substrate (see Figures 3B and 3C). Next, we checked whether the depletion of the NAD cap on U1 RNA in HIV-1-infected cells is not caused by the upregulation of DXO or Nudt12 upon infection; however, Western blot and RT–qPCR analysis showed that the levels of DXO are similar in the control and HIV-1-infected cells (see Figures S8A and S8B). The Nudt12 was not detectable in any of these samples by RT–qPCR (Figure S8B).

Using lentiviral vectors, we prepared stable MT4 cell lines in which the DXO gene was either overexpressed (MT4–DXO OE) or downregulated (MT4–DXO KD). Indeed, overexpression of DXO led to a substantial increase in the levels of the enzyme in MT4–DXO OE cells (see Figure 3D, as well as Figure S9A), whereas DXO was almost completely diminished in MT4–DXO KD cells.

Furthermore, we infected MT4–DXO OE and MT4–DXO KD cells with HIV-1, and after 4 days, we evaluated the effect of DXO expression on HIV-1 infectivity by determining the titer of HIV-1 (Figure 3E). The infectivity of HIV-1 in MT4–DXO KD cells was comparable to that in control MT4 cells (Figure S9B). By contrast, the overexpression of the NAD–RNA decapping enzyme DXO led to an increase in the infectivity of HIV-1, in comparison with control cells (Figure 3E).

We also followed the effect of DXO overexpression and knockdown on the level of NAD RNA capping in the sRNA fraction (Figure 3F and Figure S9C). We quantified the extent of NAD RNA capping in MT4–DXO OE and MT4–DXO KD cells by LC–MS (Figure S10A–C). Surprisingly, however, the extent of NAD capping of RNA isolated from MT4–DXO KD cells was lower than in the control cells. One possible explanation might reside in the redundancy of decapping enzymes in general, which was previously described.^{39,40} To support this hypothesis, we performed RT–qPCR of NudIX enzymes known to cleave NAD–RNA (Nudt12, Nudt16) or cleaving free NAD or NADH (Nudt13,⁴¹ Nudt14,³⁹ and Nudt7⁴²) (Figure S11). Potentially, some NudIXes may take over the function of the downregulated enzyme DXO and decap NAD–RNA. Surprisingly, Nudt12 was not expressed at all under either of the conditions (control and DXO KD). The expression levels of the other enzymes were not significantly changed upon the knockdown of DXO. Therefore, we concluded that some unknown decapping enzyme should be activated and cleave NAD from RNA in DXO KD. On the other hand, overexpression of the decapping enzyme DXO led to a more than six-fold decrease in the level of NAD capping of sRNA (Figure 3F). Because we observed a decrease of NAD capping in U1 RNA from HIV-1-infected cells in NAD captureSeq and LC–MS experiments and because U1 is

important for HIV-1 infection, we were interested in knowing whether manipulated levels of DXO influence the NAD capping of this RNA. We observed a statistically nonsignificant decrease in NAD capping of U1 in MT4–DXO OE cells and an increase in MT4 DXO KD cells (see Figure 3G, as well as Figures S9D and S12A–S12C). Together with the results on HIV-1 infectivity, these data suggest that overexpression of the DXO enzyme promotes HIV-1 replication through decreasing the level of NAD RNA capping. The result also indicates that the reduction of the NAD RNA cap increases HIV-1 production and that NAD-capped RNAs might play a role in antiviral defense.

In summary, we demonstrate that HIV-1 infection influences not only the total cellular NAD pool but also the NAD RNA capping of specific snRNAs (U1, U4ATAC, U5E, and U7) and snoRNAs (SNORD3G, SNORD102, SNORA50A, and SNORD3B). Since U1 plays an important role in HIV-1 infection by binding to HIV-1 pre-mRNA, we investigated the capability of the NAD RNA cap to contribute to U1 RNA and HIV-1 pre-mRNA duplex formation. The presence of NAD on U1 leads to less stable RNA–RNA duplexes, compared with TMG-capped U1. Additionally, we demonstrate that general NAD RNA capping is unfavorable for HIV-1 infection, as overexpression of the NAD decapping enzyme DXO results in decreased NAD capping and higher viral infectivity. Our work may provide an explanation for the finding that a polymorphism within the 5′ UTR region of the DXO gene in an African-American cohort of HIV-1 patients²² is associated with an altered response to HIV-1 infection. Even though the mutation in the 5′ UTR region does not influence the protein sequence itself, it may influence the stability or translatability of RNA and thus the intracellular level of the DXO protein, which, in turn, alters the efficiency of HIV-1 replication. In conclusion, we hypothesize that NAD-capped sRNAs inhibit HIV-1 replication and that part of the virus's strategy to overcome this inhibition is to reduce the pool of NAD-capped RNA. RNA modifications such as 6-methyladenosine⁴³ and 2′-O-methylation⁴⁴ of the HIV-1 genomic RNA were found to play an important role in HIV-1 infection. Therefore, the NAD cap might be another crucial RNA modification. It is present on host RNAs, influenced by the infection, and it has an impact on the viral infection itself. Moreover, we (and others) have also observed the depletion of total cellular NAD in other viral infections: severe acute respiratory syndrome coronavirus 2 (SARS-CoV-2)⁴⁵ and Herpes Simplex Virus (HSV-1) (Figure S13) from different classes of viruses than retroviruses. It would be intriguing to study whether the change in total NAD results in a change of NAD capping on the same or similar RNAs as in the case of HIV-1, and whether the presence of the NAD cap negatively influences the viral infection. If it is a general mechanism, exploiting NAD-capped RNA for therapeutic purposes might present a future avenue of antiviral treatment.

■ ASSOCIATED CONTENT

SI Supporting Information

The Supporting Information is available free of charge at <https://pubs.acs.org/doi/10.1021/acscchembio.4c00151>.

Supplementary figures and data tables (PDF)

Sequencing data are accessible in the GEO database under accession GSE191019 (XLSX)

AUTHOR INFORMATION

Corresponding Author

Hana Cahova – Institute of Organic Chemistry and Biochemistry of the CAS, 160 00 Prague 6, Czechia; orcid.org/0000-0002-4986-7858; Phone: +420 220 183 124; Email: cahova@uochb.cas.cz

Authors

Barbora Benoni – Institute of Organic Chemistry and Biochemistry of the CAS, 160 00 Prague 6, Czechia; First Faculty of Medicine, Charles University, 121 08 Prague, Czechia

Jiří František Potužník – Institute of Organic Chemistry and Biochemistry of the CAS, 160 00 Prague 6, Czechia; Faculty of Science, Department of Cell Biology, Charles University, 121 08 Prague 2, Czechia

Anton Škríba – Institute of Organic Chemistry and Biochemistry of the CAS, 160 00 Prague 6, Czechia

Roberto Benoni – Institute of Organic Chemistry and Biochemistry of the CAS, 160 00 Prague 6, Czechia

Jana Trylčová – Institute of Organic Chemistry and Biochemistry of the CAS, 160 00 Prague 6, Czechia

Matouš Tulpa – Institute of Organic Chemistry and Biochemistry of the CAS, 160 00 Prague 6, Czechia; Faculty of Science, Department of Physical and Macromolecular Chemistry, Charles University, 121 08 Prague 2, Czechia

Kristína Spustová – Institute of Organic Chemistry and Biochemistry of the CAS, 160 00 Prague 6, Czechia

Katarzyna Grab – Division of Biophysics, Faculty of Physics, University of Warsaw, 02-093 Warsaw, Poland

Maria-Bianca Mititelu – Institute of Organic Chemistry and Biochemistry of the CAS, 160 00 Prague 6, Czechia; Faculty of Science, Department of Cell Biology, Charles University, 121 08 Prague 2, Czechia

Jan Pačes – Institute of Molecular Genetics of the Czech Academy of Sciences, 142 20 Prague 4, Czechia

Jan Weber – Institute of Organic Chemistry and Biochemistry of the CAS, 160 00 Prague 6, Czechia; orcid.org/0000-0002-2799-7352

David Stanek – Institute of Molecular Genetics of the Czech Academy of Sciences, 142 20 Prague 4, Czechia

Joanna Kowalska – Division of Biophysics, Faculty of Physics, University of Warsaw, 02-093 Warsaw, Poland;

orcid.org/0000-0002-9174-7999

Lucie Bednarova – Institute of Organic Chemistry and Biochemistry of the CAS, 160 00 Prague 6, Czechia

Zuzana Keckesova – Institute of Organic Chemistry and Biochemistry of the CAS, 160 00 Prague 6, Czechia

Pavel Vopalensky – Institute of Organic Chemistry and Biochemistry of the CAS, 160 00 Prague 6, Czechia

Lenka Gahurova – Institute of Organic Chemistry and Biochemistry of the CAS, 160 00 Prague 6, Czechia; Department of Molecular Biology and Genetics, Faculty of Science, University of South Bohemia, 37005 České Budějovice, Czechia

Complete contact information is available at:

<https://pubs.acs.org/10.1021/acschembio.4c00151>

Author Contributions

B. B., A.Š., P.V., and H.C. designed the experiments and coordinated the project. J.P., J.W., and D.S. participated in the design of the experiments. B.B., J.F.P., A.Š., P.V., R.B., J.T.M.T., K.S., K.G., M.-B.M., L.B., and H.C. performed the

experiments. K.G. and J.K. prepared TMG and coordinated the chemical synthesis. L.B. measured CD spectra. Z.K. and P.V. designed and coordinated the preparation of OE and KD DXO. L.G. performed all bioinformatic analyses. H.C. supervised the work. P.V., B.B., and H.C. wrote the paper.

Notes

The authors declare no competing financial interest.

ACKNOWLEDGMENTS


We are grateful to all members of the Cahova Group for their help and advice, particularly Z. Buchová for her help with the preparation of the DXO enzyme. We acknowledge funding from the Ministry of Education, Youth and Sports of the Czech Republic, programme ERC CZ (No. LL1603), the European Research Council Executive Agency (ERCEA) under the European Union's Horizon Europe Framework Programme for Research and Innovation (Grant Agreement No. 101041374 – StressRNAction) and the Operational Programme Johannes Amos Comenius (OP JAC) project RNA for Therapy, Reg. No. CZ.02.01.01/00/22_008/0004575 co-financed by the EU. D.S. and H.C. acknowledge support from the Czech Science Foundation (Project No. 24-11157S). Computational resources were supplied by the project 'e-Infrastruktura CZ' (e-INFRA CZ LM2018140) supported by the Ministry of Education, Youth and Sports of the Czech Republic.

REFERENCES

- (1) Boccaletto, P.; Machnicka, M. A.; Purta, E.; Piątkowski, P.; Bagiński, B.; Wirecki, T. K.; de Crécy-Lagard, V.; Ross, R.; Limbach, P. A.; Kotter, A.; Helm, M.; Bujnicki, J. M. MODOMICS: a database of RNA modification pathways. 2017 update. *Nucleic Acids Res.* **2018**, *46*, D303–D307.
- (2) Chen, Y. G.; Kowtoniuk, W. E.; Agarwal, I.; Shen, Y.; Liu, D. R. LC/MS analysis of cellular RNA reveals NAD-linked RNA. *Nat. Chem. Biol.* **2009**, *5*, 879.
- (3) Sherwood, A. V.; Rivera-Rangel, L. R.; Ryberg, L. A.; Larsen, H. S.; Anker, K. M.; Costa, R.; Vågbo, C. B.; Jakljević, E.; Pham, L. V.; Fernandez-Antunez, C.; Indrisiunaite, G.; Podolska-Charlery, A.; Grothen, J. E. R.; Langvad, N. W.; Fossat, N.; Offersgaard, A.; Al-Chaer, A.; Nielsen, L.; Kuśnierczyk, A.; Sølund, C.; Weis, N.; Gottwein, J. M.; Holmbeck, K.; Bottaro, S.; Ramirez, S.; Bukh, J.; Scheel, T. K. H.; Vinther, J. Hepatitis C virus RNA is 5'-capped with flavin adenine dinucleotide. *Nature* **2023**, *619*, 811–818.
- (4) Hudeček, O.; Benoni, R.; Reyes-Gutierrez, P. E.; Culka, M.; Šanderová, H.; Hubálek, M.; Rulíšek, L.; Cvačka, J.; Krásný, L.; Cahová, H. Dinucleoside polyphosphates act as 5'-RNA caps in bacteria. *Nat. Commun.* **2020**, *11*, 1052.
- (5) František Potužník, J.; Nešuta, O.; Škríba, A.; Voleníková, B.; Mititelu, M.-B.; Mancini, F.; Serianini, V.; Fernandez, H.; Spustová, K.; Trylčová, J.; Vopalensky, P.; Cahová, H. Diadenosine Tetraphosphate (Ap₄A) Serves as a 5' RNA Cap in Mammalian Cells. *Angew. Chem., Int. Ed.* **2024**, *63*, e202314951.
- (6) Cahova, H.; Winz, M.-L.; Hofer, K.; Nuebel, G.; Jaeschke, A. NAD captureSeq indicates NAD as a bacterial cap for a subset of regulatory RNAs. *Nature* **2015**, *519*, 374.
- (7) Winz, M.-L.; Cahová, H.; Nübel, G.; Frindert, J.; Höfer, K.; Jäschke, A. Capture and sequencing of NAD-capped RNA sequences with NAD captureSeq. *Nat. Protoc.* **2017**, *12*, 122.
- (8) Hu, H.; Flynn, N.; Zhang, H.; You, C.; Hang, R.; Wang, X.; Zhong, H.; Chan, Z.; Xia, Y.; Chen, X. (2021) SPAAC-NAD-seq, a sensitive and accurate method to profile NAD(+) capped transcripts, *Proc. Natl. Acad. Sci. U.S.A.* **118**, DOI: [10.1073/pnas.2025595118](https://doi.org/10.1073/pnas.2025595118).
- (9) Sharma, S.; Yang, J.; Favate, J.; Shah, P.; Kiledjian, M. NADcapPro and circNC: methods for accurate profiling of NAD and non-canonical RNA caps in eukaryotes. *Commun. Biol.* **2023**, *6*, 406.



- (10) Niu, K.; Zhang, J.; Ge, S.; Li, D.; Sun, K.; You, Y.; Qiu, J.; Wang, K.; Wang, X.; Liu, R.; Liu, Y.; Li, B.; Zhu, Z. J.; Qu, L.; Jiang, H.; Liu, N. ONE-seq: epitranscriptome and gene-specific profiling of NAD-capped RNA. *Nucleic Acids Res.* **2023**, *51*, No. e12.
- (11) Morales-Filloy, H. G.; Zhang, Y.; Nübel, G.; George, S. E.; Korn, N.; Wolz, C.; Jäschke, A. The 5'-NAD cap of RNAPIII modulates toxin production in *Staphylococcus aureus* isolates. *J. Bacteriol.* **2020**, *202*, e00591-19.
- (12) Walters, R. W.; Matheny, T.; Mizoue, L. S.; Rao, B. S.; Muhlrad, D.; Parker, R. Identification of NAD⁺ capped mRNAs in *Saccharomyces cerevisiae*. *Proc. Natl. Acad. Sci. U.S.A.* **2017**, *114*, 480–485.
- (13) Jiao, X.; Doamekpor, S. K.; Bird, J. G.; Nickels, B. E.; Tong, L.; Hart, R. P.; Kiledjian, M. 5' End Nicotinamide Adenine Dinucleotide Cap in Human Cells Promotes RNA Decay through DXO-Mediated deNADding. *Cell* **2017**, *168*, 1015–1027.e10.
- (14) Wolfram-Schauerte, M.; Höfer, K. NAD-capped RNAs – a redox cofactor meets RNA. *Trends Biochem. Sci.* **2023**, *48*, 142–155.
- (15) Wolfram-Schauerte, M.; Pozhydaeva, N.; Grawenhoff, J.; Welp, L. M.; Silbern, I.; Wulf, A.; Billau, F. A.; Glatter, T.; Urlaub, H.; Jäschke, A.; Höfer, K. A viral ADP-ribosyltransferase attaches RNA chains to host proteins. *Nature* **2023**, *620*, 1054–1062.
- (16) Murray, M. F.; Nghiem, M.; Srinivasan, A. HIV infection decreases intracellular nicotinamide adenine dinucleotide [NAD]. *Biochem. Biophys. Res. Commun.* **1995**, *212*, 126–131.
- (17) Rodríguez-Alba, J. C.; Abrego-Peredo, A.; Gallardo-Hernández, C.; Pérez-Lara, J.; Santiago-Cruz, W.; Jiang, W.; Espinosa, E. HIV Disease Progression: Overexpression of the Ectoenzyme CD38 as a Contributory Factor? *Bioessays* **2019**, *41*, e1800128.
- (18) Taylor, E. W. The oxidative stress-induced niacin sink (OSINS) model for HIV pathogenesis. *Toxicology* **2010**, *278*, 124–130.
- (19) Furlini, G.; Re, M. C.; La Placa, M. Increased poly(ADP-ribose)polymerase activity in cells infected by human immunodeficiency virus type-1. *Microbiologica* **1991**, *14*, 141–148.
- (20) Murray, M. F.; Srinivasan, A. Nicotinamide inhibits HIV-1 in both acute and chronic in vitro infection. *Biochem. Biophys. Res. Commun.* **1995**, *210*, 954–959.
- (21) Murray, M. F. Nicotinamide: an oral antimicrobial agent with activity against both *Mycobacterium tuberculosis* and human immunodeficiency virus. *Clin. Infect. Dis.* **2003**, *36*, 453–460.
- (22) Pelak, K.; Goldstein, D. B.; Walley, N. M.; Fellay, J.; Ge, D.; Shianna, K. V.; Gumbs, C.; Gao, X.; Maia, J. M.; Cronin, K. D.; et al. Host determinants of HIV-1 control in African Americans. *J. Infect. Dis.* **2010**, *201*, 1141–1149.
- (23) Lu, X. B.; Heimer, J.; Rekosch, D.; Hammarskjöld, M. L. U1 small nuclear RNA plays a direct role in the formation of a rev-regulated human immunodeficiency virus env mRNA that remains unspliced. *Proc. Natl. Acad. Sci. U.S.A.* **1990**, *87*, 7598–7602.
- (24) Mandal, D.; Feng, Z.; Stoltzfus, C. M. Excessive RNA splicing and inhibition of HIV-1 replication induced by modified U1 small nuclear RNAs. *J. Virol.* **2010**, *84*, 12790–12800.
- (25) Hamm, J.; Darzynkiewicz, E.; Tahara, S. M.; Mattaj, I. W. The trimethylguanosine cap structure of U1 snRNA is a component of a bipartite nuclear targeting signal. *Cell* **1990**, *62*, 569–577.
- (26) Bird, J. G.; Zhang, Y.; Tian, Y.; Panova, N.; Barvik, I.; Greene, L.; Liu, M.; Buckley, B.; Krásný, L.; Lee, J. K.; Kaplan, C. D.; Ebright, R. H.; Nickels, B. E. The mechanism of RNA 5' capping with NAD⁺, NADH and desphospho-CoA. *Nature* **2016**, *535*, 444.
- (27) Wilusz, J. Putting an 'End' to HIV mRNAs: capping and polyadenylation as potential therapeutic targets. *AIDS Res. Therapy* **2013**, *10*, 31.
- (28) Eckwahl, M. J.; Arnion, H.; Kharytonchyk, S.; Zang, T.; Bieniasz, P. D.; Telesnitsky, A.; Wolin, S. L. Analysis of the human immunodeficiency virus-1 RNA packageome. *RNA* **2016**, *22*, 1228.
- (29) Šimonová, A.; Svojanovská, B.; Trylčová, J.; Hubálek, M.; Moravčík, O.; Závřel, M.; Pávová, M.; Hodek, J.; Weber, J.; Cvačka, J.; Pačes, J.; Cahová, H. LC/MS analysis and deep sequencing reveal the accurate RNA composition in the HIV-1 virion. *Sci. Rep.* **2019**, *9*, 8697.
- (30) Frindert, J.; Zhang, Y.; Nübel, G.; Kahloon, M.; Kolmar, L.; Hotz-Wagenblatt, A.; Burhenne, J.; Haefeli, W. E.; Jäschke, A. Identification, Biosynthesis, and Decapping of NAD-Capped RNAs in *B. subtilis*. *Cell Rep.* **2018**, *24*, 1890–1901.e1898.
- (31) Sajic, R.; Lee, K.; Asai, K.; Sakac, D.; Branch, D. R.; Upton, C.; Cochrane, A. Use of modified U1 snRNAs to inhibit HIV-1 replication. *Nucleic Acids Res.* **2006**, *35*, 247–255.
- (32) Benoni, R.; Culka, M.; Hudeček, O.; Gahurova, L.; Cahová, H. Dinucleoside Polyphosphates as RNA Building Blocks with Pairing Ability in Transcription Initiation. *ACS Chem. Biol.* **2020**, *15*, 1765–1772.
- (33) Auffinger, P.; Westhof, E. (1998) Effects of Pseudouridylation on tRNA Hydration and Dynamics: A Theoretical Approach. In *Modification and Editing of RNA*, pp 103–112.
- (34) Newby, M. I.; Greenbaum, N. L. A conserved pseudouridine modification in eukaryotic U2 snRNA induces a change in branch-site architecture. *RNA* **2001**, *7*, 833–845.
- (35) Grudzien-Nogalska, E.; Wu, Y.; Jiao, X.; Cui, H.; Mateyak, M. K.; Hart, R. P.; Tong, L.; Kiledjian, M. Structural and mechanistic basis of mammalian Nudt12 RNA deNADding. *Nat. Chem. Biol.* **2019**, *15*, 575–582.
- (36) Sharma, S.; Grudzien-Nogalska, E.; Hamilton, K.; Jiao, X.; Yang, J.; Tong, L.; Kiledjian, M. Mammalian Nudix proteins cleave nucleotide metabolite caps on RNAs. *Nucleic Acids Res.* **2020**, *48*, 6788–6798.
- (37) Abdelraheim, S. R.; Spiller, D. G.; McLennan, A. G. Mammalian NADH diphosphatases of the Nudix family: cloning and characterization of the human peroxisomal NUDT12 protein. *Biochem. J.* **2003**, *374*, 329–335.
- (38) Jiao, X.; Chang, J. H.; Kilic, T.; Tong, L.; Kiledjian, M. A mammalian pre-mRNA 5' end capping quality control mechanism and an unexpected link of capping to pre-mRNA processing. *Mol. Cell* **2013**, *50*, 104–115.
- (39) Carreras-Puigvert, J.; Zitnik, M.; Jemth, A. S.; Carter, M.; Unterlass, J. E.; Hallström, B.; Loseva, O.; Karem, Z.; Calderón-Montaño, J. M.; Lindskog, C.; et al. A comprehensive structural, biochemical and biological profiling of the human NUDIX hydrolase family. *Nat. Commun.* **2017**, *8*, 1541.
- (40) Li, Y.; Song, M.; Kiledjian, M. Differential utilization of decapping enzymes in mammalian mRNA decay pathways. *RNA* **2011**, *17*, 419–428.
- (41) Abdelraheim, S. R.; Spiller, D. G.; McLennan, A. G. Mouse Nudt13 is a Mitochondrial Nudix Hydrolase with NAD(P)H Pyrophosphohydrolase Activity. *Protein J.* **2017**, *36*, 425–432.
- (42) Duarte-Pereira, S.; Matos, S.; Oliveira, J. L.; Silva, R. M. Study of NAD-interacting proteins highlights the extent of NAD regulatory roles in the cell and its potential as a therapeutic target. *J. Integr. Bioinform.* **2023**, *20*, 20220049.
- (43) Baek, A.; Lee, G.-E.; Golconda, S.; Rayhan, A.; Manganaris, A. A.; Chen, S.; Tirumuru, N.; Yu, H.; Kim, S.; Kimmel, C.; Zablocki, O.; Sullivan, M. B.; Addepalli, B.; Wu, L.; Kim, S. Single-molecule epitranscriptomic analysis of full-length HIV-1 RNAs reveals functional roles of site-specific m6As. *Nat. Microbiol.* **2024**, *9*, 1340.
- (44) Ringard, M.; Marchand, V.; Decroly, E.; Motorin, Y.; Bennasser, Y. FTSJ3 is an RNA 2'-O-methyltransferase recruited by HIV to avoid innate immune sensing. *Nature* **2019**, *565*, S00–S04.
- (45) Brenner, C. Viral infection as an NAD⁺ battlefield. *Nat. Metab.* **2022**, *4*, 2–3.

SCIENTIFIC REPORTS



OPEN

LC/MS analysis and deep sequencing reveal the accurate RNA composition in the HIV-1 virion

Anna Šimonová^{1,2}, Barbora Svojanovská^{1,2}, Jana Trylčová¹, Martin Hubálek¹, Ondřej Moravčík³, Martin Zavřel¹, Marcela Pávová¹, Jan Hodek¹, Jan Weber¹ , Josef Cvačka¹, Jan Pačes^{1,3,4} & Hana Cahová¹ 

The mechanism of action of various viruses has been the primary focus of many studies. Yet, the data on RNA modifications in any type of virus are scarce. Methods for the sensitive analysis of RNA modifications have been developed only recently and they have not been applied to viruses. In particular, the RNA composition of HIV-1 virions has never been determined with sufficiently exact methods. Here, we reveal that the RNA of HIV-1 virions contains surprisingly high amount of the 1-methyladenosine. We are the first to use a liquid chromatography-mass spectrometry analysis (LC/MS) of virion RNA, which we combined with m¹A profiling and deep sequencing. We found that m¹A was present in the tRNA, but not in the genomic HIV-1 RNA and the abundant 7SL RNA. We were able to calculate that an HIV-1 virion contains per 2 copies of genomic RNA and 14 copies of 7SL RNA also 770 copies of tRNA, which is approximately 10 times more than thus far expected. These new insights into the composition of the HIV-1 virion can help in future studies to identify the role of nonprimer tRNAs in retroviruses. Moreover, we present a promising new tool for studying the compositions of virions.

To date, more than 140 chemical RNA modifications are known¹. Chemical RNA modification expand the repertoire of four natural nucleosides and influence RNA structure and function. The majority has been found in highly concentrated RNA moieties such as ribosomal (rRNA) or transfer RNA (tRNA). Nevertheless, there is growing evidence that coding messenger RNA (mRNA) and regulatory RNA also contain various chemical modifications². Their existence in mRNA is complicated to be proved by common LC/MS technique but special and selective profiling or capturing techniques for various RNA modification have been developed lately. In particular, pseudouridine has been found in the mRNA thanks to the development of the selective profiling techniques Pseudo-seq³ and Ψ-seq⁴. Also, the widespread presence of 5-methylcytosine across the human transcriptome has been demonstrated by a bisulphite technique combined with deep sequencing⁵. A to I editing of the mRNA has been confirmed by Inosine chemical erasing⁶. The NAD captureSeq⁷ allowed identification of RNAs with covalently attached Nicotinamide adenine dinucleotide (NAD) at 5' end. So far, this method has enabled the detection of NAD in sRNA, and mRNA in *E. coli*⁷ and in eukaryotes^{8,9}.

The development of a profiling technique for 6-methyladenosine (m⁶A) in mRNA^{10,11} paved the way for the emerging field of epitranscriptomic. Another common epitranscriptomic mark in mRNA was supposed to be 1-methyladenosine (m¹A)^{12,13}. As well as for m⁶A detection the specific antibodies have been used to detect m¹A in the human transcriptome. The problem of immunoprecipitation methods is that they do not allow for single base resolution of particular RNA modification. The authors claimed identification of thousands of transcripts bearing m¹A in eukaryotic cells. A subsequent study indicated that the m¹A is only present in 15 sites of the mRNA, in the previously known T-loop of tRNAs, and in rRNA from HEK293T cells¹⁴. Apart from

¹Institute of Organic Chemistry and Biochemistry of the Czech Academy of Sciences, Prague, 16610, Czech Republic.

²First Faculty of Medicine, Charles University, Prague, 12108, Czech Republic. ³Institute of Molecular Genetics of the Czech Academy of Sciences, Prague, 14220, Czech Republic. ⁴University of Chemistry and Technology, Prague, 16628, Czech Republic. Correspondence and requests for materials should be addressed to H.C. (email: cahova@uochb.cas.cz)

immunoprecipitation, the authors of the later method employed two types of reverse transcriptases enabling single-base resolution.

The study of the chemical structures of RNA species such as mRNA, micro RNA and guiding RNA is hampered by their very low concentrations in cells. Therefore, we believe that viruses may represent a suitable model system for RNA modification studies because they have simple intrinsic structure and well-known molecular mechanisms.

So far, m⁶A profiling is the only applied technique for the studies of viral RNA modifications. Recently, m⁶A profiling has been used to study m⁶A in the genomic RNA of *Flaviviridae*¹⁵. In particular, the conserved regions modified by m⁶A were identified in genomic RNA of hepatitis C (HCV), dengue, Zika, yellow fever and West Nile virus. The m⁶A modulated infection by HCV and the depletion of m⁶A methyltransferases or m⁶A demethylase was found to increase or decrease the HCV particle production, respectively. A photo-crosslinking-assisted m⁶A sequencing technique was used to precisely map m⁶A editing sites on the HIV-1 genome¹⁶. The m⁶A sites were found to cluster in the HIV-1 3' untranslated region and to recruit YTHDF “reader” proteins. The m⁶A editing and the recruitment of YTHDF proteins were identified as the positive regulators of HIV-1 mRNA expression.

As new layers of RNA modifications are constantly being uncovered in the transcriptome, we can presume that other RNA modifications besides m⁶A can be employed by viruses. At first, we focused on the viral packageome of HIV-1. It was believed that HIV-1 packs in virion not only two copies of genomic RNA, but also 12–14 copies of guiding 7SL RNA^{17,18}, 8 copies of tRNA^{Lys3} that serve as primer for its reverse transcriptase^{19–21}, around 12 copies of tRNA^{Lys1,2}, around 50 copies of rather randomly packed tRNAs and some fragments of other mRNA, rRNA etc^{18,22–26}. In total, the host cell-derived RNA should comprise up to half of the virion RNA by mass^{27,28}.

To best of our knowledge, the LC/MS analysis of RNA from viral particles has not been reported yet. We isolated RNA from HIV-1 viral particles, digested it into form of nucleosides and we analysed this mixture by LC/MS system. We found surprisingly high amount of m¹A (4.1% of all adenosines - A) in the packageomic RNA that corresponded to approximately 340 1-methyladenosines (Supplementary Table S1). The tRNA molecules contain one m¹A in their sequence, what correlates to 70 positions. In the light of the emerging field of epitranscriptomics we asked the question where the rest 270 m¹A can come from and whether the genomic HIV-1 RNA or other co-packed RNA are so heavily methylated. Therefore, we prepared four deep sequencing libraries with particular focus on m¹A profiling. We found that the m¹A is present solely in tRNA and that genomic HIV-1 RNA, neither 7SL RNA do not contain this modification. Based on this results we could recalculate the ratios of genomic HIV-1 RNA, 7SL RNA and tRNAs in the virion. We concluded that the HIV-1 virion consists beside 2 copies of genomic HIV-1 RNA and 14 copies of 7SL RNA also 770 copies of tRNA. Our results suggest the role for the cellular RNA could be much more significant than expected so far, both in mechanism of viral infection and in viral replication. Our study also confirms the evidence that the m¹A modification is rather typical for tRNAs¹⁴ and it is not so widespread as it was previously described¹². We also show here that the LC/MS analysis of RNA modifications in virion in combination with deep sequencing can be used for the determination of the exact RNA composition of complex virions. The presence of specific RNA modification m¹A helped us to bring new insight into the HIV-1 virion composition. In future, this method can be applied also for studies of the composition of other viruses.

Results

LC/MS technique reveals a higher amount of m¹A in the HIV-1 packageome than expected. In order to analyse the RNA modifications in the HIV-1 virus, we firstly produced HIV-1 virus by infection of MT4 cells (Fig. 1A). We harvested the supernatant both from the infected cells and the uninfected MT4 cells, and we used the latter as the mock medium. After purification of the virions on sucrose cushion, we treated the sample by RNase and DNase to digest the nucleic acids not packed in viral particles. Then, the RNA was isolated by RNazol. The samples were precipitated using ethanol and then digested by Nuclease P1 and Alkaline Phosphatase to form nucleosides. The digested RNA was analysed using a Synapt G2 LC/MS system (Fig. 1A,B). The authenticity of the methylated nucleosides was confirmed by injection of synthetic standards, which produced the same *m/z* signal and were eluted at the same time.

Using LC/MS analysis, we observed methylated adenosines. m⁶A was present only in low amount approx. 1.1%. Surprisingly, we found quite high amount of m¹A around 4.1% of all adenosines in the packageome of the HIV-1-virus. We also searched for other known modified adenosines in the RNA digest and we were able to confirm only N⁶-threonylcarbamoyladenine (t⁶A), 2'-O-methyladenosine (Am) and 2-methylthio-N⁶-threonylcarbamoyladenine (mS²t⁶A) (Supplementary Figures S1, S2). Other modified adenosines were not detected by our LC/MS analysis or they were present only in traces that we could not calculate (2-methylthio-N⁶-isopentenyladenosine, N⁶-(cis-hydroxyisopentenyl)adenosine, N⁶-isopentenyladenosine, Supplementary Table S2²⁹). Analysing the synthetic standards of m⁶A, m¹A, Am and t⁶A, we were able to extrapolate their proportional representation in the digest (Supplementary Figures S1, S2, Table S3). As we did not have available standard of mS²t⁶A, we presume that the molecule has similar ionization properties as t⁶A. The packageomic RNA contains 4.1% of m¹A, 1.1% of m⁶A, 0.9% of Am, 3.2% of t⁶A and 1.5% of mS²t⁶A (rest is A).

To verify that the signals of modified nucleosides originate from RNA molecules packed in viral particles, we analyzed the medium of the uninfected cells by LC/MS analysis (Supplementary Table S4). Here, we did not detect any traces of m¹A or other modified A. Thus, we conclude that the signals of modified nucleosides in the samples prepared from supernatant of HIV-1 infected cells stem indeed from RNA molecules packed in viral particles. As the RNazol protocol only isolates oligonucleotides longer than 10 nt, we can rule out the possibility that the modified nucleoside signal originates from co-packed small molecules.

Using previously published data on the number of co-packed RNA entities in one particle (two genomic HIV-1 RNAs, 14 7SL RNAs, approx. 70 tRNAs, Fig. 1C)^{18,22,23} and previous evidence on the presence of m¹A in position 58 of the majority of tRNAs, we conclude that in RNA packed in a viral particle, 270 positions would be methylated. However, this number did not correspond to the previous estimate of approximately 70 tRNA molecules.

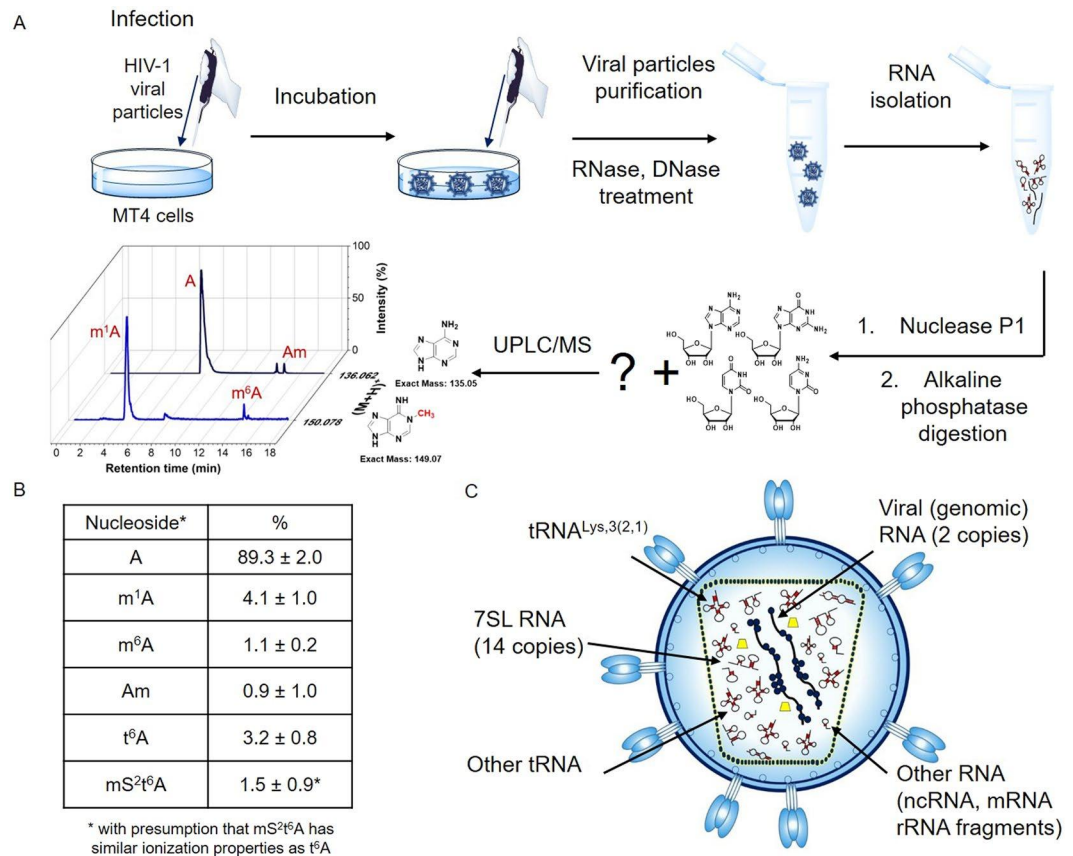


Figure 1. LC/MS analysis of RNA in the HIV-1 packageome. **(A)** Scheme showing the preparation of HIV-1 samples for LC/MS analysis. **(B)** Ratios of nucleosides in the HIV-1 samples as analysed by LC/MS using biological tetraplicates. **(C)** A schematic view on the RNA composition in HIV-1.

m¹A is solely present in the tRNA. To investigate the exact positions of m¹A in the packageomic RNA, we prepared a deep sequencing library. As the viral packageome is very simple, we used for the m¹A localisation the method based on the reverse transcription signature^{30–32}. The RNA for deep sequencing was prepared in biological triplicates. Every sample was divided in two parts and one part was treated by basic conditions to obtain an m¹A conversion to m⁶A (Dimroth rearrangement)¹² that is normally read as A by reverse transcriptase. We prepared three deep sequencing libraries using SuperScript™ III reverse transcriptase, which should either mis-read m¹A or arrest meeting m¹A. One deep sequencing library was prepared with TGIRT™ reverse transcriptase, which should confirm the m¹A position at base resolution.

In the deep sequencing protocol (Fig. 2A), we used a sequence of the following steps: The RNA was first fragmented to obtain fragments of uniform lengths (approx. 100 nt), then ligated with the first adaptor, reverse transcribed, tailed by cytidine triphosphate (CTP) and finally ligated with the second adaptor. After PCR with indexed primers, the samples were separated using agarose gel electrophoresis. The cut off was approximately 100–350 nt including the adaptors. Afterwards, the samples were pooled in a library and sequenced by IonTorrent technology.

The bioinformatics analysis confirmed that the virion contains mainly tRNAs, 7SL RNA and HIV-1 genomic RNA (Fig. 2C, Supplementary Table S5). Any other cellular RNAs were not detected in significant amount (more than 0.1%). By analysing the deep sequencing data using bioinformatics we identified m¹A in position 58 of tRNA^{Lys} TTT-3.1, tRNA^{Lys} CTT-2.1, tRNA^{Lys} CTT-1.1, and tRNA^{Asn} GTT-2.1, as well as in position 9 of tRNA^{Asp} GTC-2.1. Based on a previous report³⁰, we expected the reverse transcriptase to be paused (observed arrest) when meeting m¹A. However, pattern of misreading for m¹A in artificial sequences read by reverse transcriptase was also reported^{30,32}. We observed this behavior of reverse transcriptase in the position 58 of some tRNAs. Approximately 70% of the m¹A in position 58^{33,34} was misread (Fig. 2B – blue colour) as G or T by both reverse transcriptases used (SuperScript™ III – library 1–3 and TGIRT™ – library 4). In the sample that was treated with basic conditions, the misreading of position 58 was only approximately 30% (Fig. 2B). This observation corresponds to the expected conversion of m¹A to m⁶A in the RNA. It also proves the chemical authenticity of m¹A because the presence of other modified A would cause misincorporation but the ratio of misreading would not change after basic treatment.

Surprisingly, m¹A in the position 9 of tRNA^{Asp} GTC-2.1, caused rather arrest (Fig. 2B – orange colour) of SuperScript™ III in approximately 85% and a misreading as T (86%) was observed only in the experiment with TGIRT™. In order to verify that the m¹A profiling method works in our hand also when long RNAs are used, we tested the protocol on 28S rRNA from HEK293T cells. In this case, we observed arrest of the reverse transcriptase

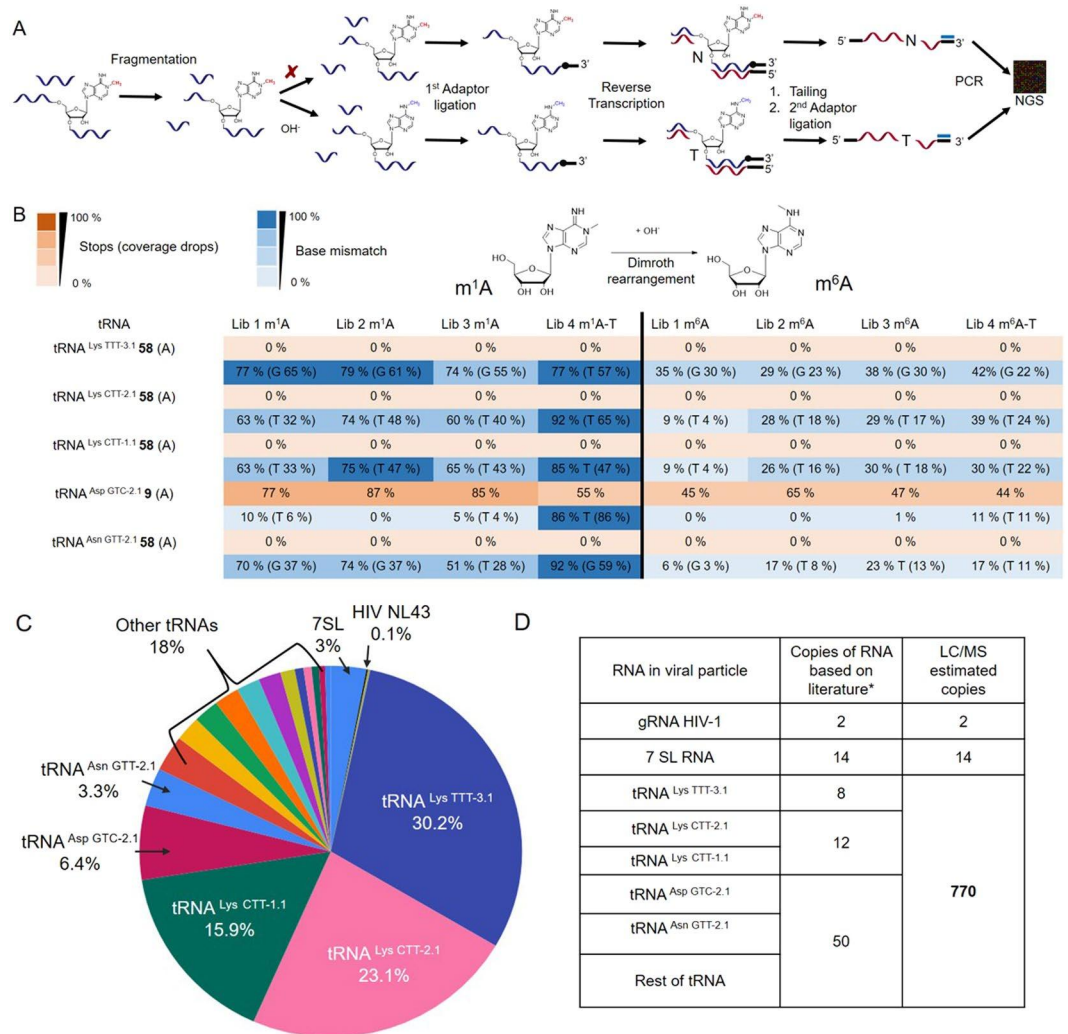


Figure 2. m¹A profiling of RNAs in HIV-1 virion. **(A)** Scheme showing the preparation of the deep sequencing libraries of RNA isolated from HIV-1 virions. **(B)** Table showing the observed misincorporation (blue) or arrests (orange) of reverse transcriptase in the deep sequencing libraries. T stands for library Lib4 prepared with TGIRT reverse transcriptase, while Lib1-Lib3 libraries were prepared with SuperScriptTM III reverse transcriptase. **(C)** The percentages of the most abundant RNA reads in the deep sequencing libraries. **(D)** Table showing the extrapolated numbers of copies of RNAs in HIV-1 virion based on literature (*^{17,18}) and on our LC/MS data.

meeting m¹A in position 1317 in 80%. This is contrary to the reverse transcriptase TGIRTTM, which misread the m¹A mainly as G in 28S rRNA (Supplementary Table S7). Our observation shows that the reverse transcriptase behavior depends strongly not only on type of RNA modification but also on sequence and 2D structure (loop, bulge etc.). In any case, the behaviour of both reverse transcriptases (either arrest or misreading) always proved the presence of m¹A.

Once we confirmed the m¹A in tRNAs co-packed in viral particle, we searched for other m¹A in all virion RNA entities. Adenosine is reported to be methylated in position 1 mainly within the specific motif GUUCNANNC¹⁴ or similar. Therefore, we looked for i) the misreading pattern, ii) the arrests of reverse transcriptase, and iii) a similar motif to GUUCNANNC (allowing one alteration) in 7SL RNA and the genomic HIV-1 RNA (Supplementary Table S7). Although we found the sequence motif allowing one alteration several times in the genomic RNA of HIV-1, we never observed a significant misreading or arresting pattern of reverse transcriptase meeting A in whole genomic RNA of HIV-1. 7SL RNA contains also one sequence motif but neither there we did not observe any significant misreading or arresting pattern. Because there are no other abundant RNA molecules beside tRNAs, (Supplementary Table S5), we concluded that all LC/MS detected m¹A originates from the co-packed tRNAs.

To exclude the possibility that the used HIV-1 particles were not sufficiently purified on the sucrose cushion and the detected RNA, thus, came from extracellular vesicles³⁵, we purified the viral particles using OptiPrep density gradient. The RNA prepared from OptiPrep density gradient purified virus represented 96% of RNA from sucrose cushion purified virus. The RNA from fractions removed by OptiPrep density gradient contained

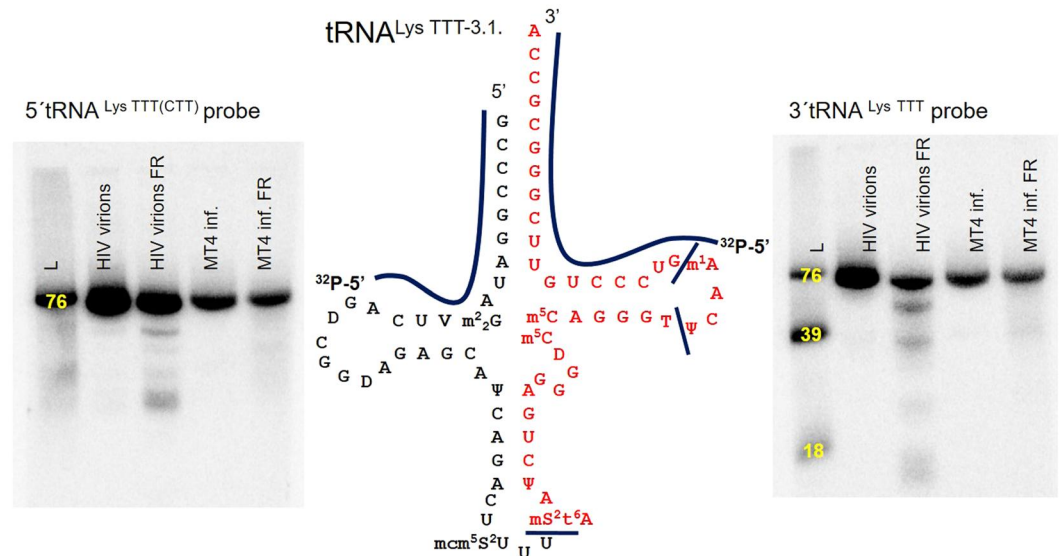


Figure 3. Northern blot analysis of RNA purified from HIV virions before and after fragmentation (FR) and from MT4 cells infected (inf.) with HIV-1 before and after fragmentation. The radioactively labelled probes were used for 5' (left panel) and 3' (right panel) ends of tRNA^{Lys} TTT-3.1. The yellow numbers stand for the size of synthetically prepared ladder (L) with the same sequence as natural tRNA^{Lys} TTT-3.1.

1000 x less HIV-1 genomic RNA (Supplementary Figure S3) and we did not observe any tRNAs using TapeStation analysis (Supplementary Figure S4A).

Based on the deep sequencing data, we can conclude that the viral particle contains more than 96% of host RNA represented mainly by tRNAs. We estimate that tRNA^{Lys} TTT-3.1 is present in 30%, tRNA^{Lys} CTT-2.1 in 23%, tRNA^{Lys} CTT-1.1 in 16%, tRNA^{Asp} GTC-2.1 in 6% and tRNA^{Asn} GTT-2.1 in 3% (Fig. 2C).

Precision of mapping is in almost all cases >99% (Supplementary Figure S5). However, the determined percent was averaged over all libraries and suffer from rather high variability. We are also aware of that e.g. PCR cycles can introduce a certain bias by preferentially amplifying short sequences over long ones.

m¹A stems from full-length tRNAs. In our deep sequencing data, we only observed the 3' half of the tRNA^{Lys} TTT-3.1. We hypothesised that this phenomenon can either be explained by the presence of a bulky RNA modification such as mS²t⁶A at the anticodon loop or by the fact that the viral particle only contains the 3'-tRNA half of the tRNA^{Lys} TTT-3.1. To shed light on this, we designed a northern blot analysis of the tRNA fragments. Radioactively labelled probes were designed for the 3' ends of tRNA^{Lys} TTT-3.1 and tRNA^{Lys} CTT-1.1 (2.1) as well as for the 5' end of tRNA^{Lys} TTT-3.1. As the 5' end of tRNA^{Lys} TTT-3.1 and tRNA^{Lys} CTT-1.1 (2.1) is similar, the 5' end probe hybridize to all three tRNAs. We also prepared ladder with the sequence of tRNA^{Lys} TTT-3.1 by *in vitro* transcription. The ladder helped us to estimate the size of observed bands. To rule out that the observed fragment in the deep sequencing data was caused by the fragmentation step, we analysed the RNA isolated from the viral particles and from the MT4 cells infected by HIV-1 before and after fragmentation. We observed the presence of 3'-tRNA fragments only in the RNA from viral particles after fragmentation (Fig. 3). Therefore, we ruled out the possibility that such 3'-tRNA fragments can contribute to the high level of m¹A. Apparently, the observed fragments were formed during the preparation of the sample and they are not naturally present in the virion. We thus conclude that m¹A solely originates from full-length tRNAs.

Nevertheless, the amount of observed m¹A did not correspond to the number of co-packed tRNAs of 70 copies total in viral particle previously published^{24–26}. Hence, we come to an end that the amount of co-packed tRNA is approximately 10-fold higher than previously reported. Based on the direct method of LC/MS analysis we can calculate that per 2 copies of genomic HIV-1 RNA and 14 copies of 7SL RNA HIV-1 virion contains also 770 copies of tRNAs (Fig. 2D, Supplementary Figure S6).

Discussion

The RNA in the packageome of the HIV-1 virus was believed to consist of 2 copies of genomic HIV-1 RNA, 14 copies of 7SL RNA and 70 copies of tRNAs. Nevertheless, so far any direct method has not been used to study the RNA composition of virions. As first, we used LC/MS to study chemical composition of packageomic RNA. Surprisingly high amount of m¹A led us to the deep sequencing analysis with particular focus on m¹A. Even though immunoprecipitation methods for mapping m¹A in complete transcriptome have been published^{12,14}, we presumed that the method based on the reverse transcription signature would be sufficient for the localisation of m¹A in simple packageome^{30,31}. m¹A profiling confirmed presence of this modification in tRNAs but excluded its presence in other RNA entities co-packed in HIV-1 virion. Once we ruled out the possibility that the m¹A can stem from tRNA fragments, we were able to recalculate ratios of RNA molecules in HIV-1 virion. Based on LC/MS analysis, we extrapolate that the virion contains per 2 molecules of genomic HIV-1 RNA and 14 copies of 7SL RNA another 770 copies of various tRNAs.

So far, only one work has dealt with a deep sequencing analysis of HIV-1 particles²⁴. According to Eckwahl *et al.*, the HIV-1 particle contain even less than 8 copies of tRNA^{Lys}_{TTT-3.1}, as was previously reported. However, Eckwahl *et al.* admit that an absence of tRNA reads in their analysis can be caused by fragmentation that would lead to fragments <50 nt. Fragmented RNA would be underrepresented in their cDNA. In our deep sequencing libraries, however, we included RNAs with a size of around 40 nt. We, therefore, did not lose those short reads. In particular, we found that tRNA^{Lys}_{TTT-3.1} caused an almost quantitative abortion of the reverse transcriptase because it contains the bulky m⁵2⁶A³⁶ in position 37. As a result, the read had a length of only 39 nt.

Our deep sequencing analysis suggests that the HIV-1 virion contains approximately 69% of three versions of tRNA^{Lys}. This is in agreement with works published by Kleiman *et al.* who found the ratio to be about 60%^{37,38}. The same group later demonstrated using both microarray and 2D Page methods that the amount of all tRNA^{Lys} is only about 45%³⁹. The reason for this difference may be imperfect labelling as both methods relied on ligation reactions.

The estimations of other co-packed tRNAs (50 molecules per virion)¹⁸ were based on the fact that the host non-coding RNAs in retroviruses outnumber viral gRNA by a factor of at least 50⁴⁰.

In other works, the quantification of further tRNAs co-packed by an HIV-1 virion was usually omitted. Based on the knowledge that every tRNA contains one m¹A in its sequence, we were able to quantify the number of all tRNAs in the viral packageome to be around 770. It is, however, important to mention that others often studied viral particles produced from different cells such as COS-7 cells^{37,38} or CEM-SS cells⁴⁰, or produced by transfection and not infection²². Those factors can influence the composition of viral particles.

A recent report on RNA modifications in viral RNA that was purified via selective probes indicates that the genomic RNA of HIV-1 can contain besides m¹A, 35 other RNA modifications⁴¹. The authors, however, conclude this fact only based on MS data, which means that the samples could be contaminated with heavily modified tRNA molecules. tRNA^{Lys}_{TTT-3.1}, for example, can be bound so tightly to gRNA that it is not possible to separate the pure genomic RNA. Another error could have been introduced in the preparation of the viral samples. As the authors used only transfection, the plasmid containing the HIV-1 genomic sequence could have been fully transcribed into RNA. Based on our screening of HIV-1 sequence, we know that the additional plasmid sequence pNL4-3 contains the original motif GUUCNANNC, which might be methylated. However, we cannot exclude that a certain position in the genomic HIV-1 is methylated from less than 5% as our profiling technique would not be able to track it. However, this amount of m¹A would not significantly contribute to the observed LC/MS signal. It is also arguable, whether such level of methylation would have any biological significance.

In our work, we also considered the existence of 3' tRNA fragments that could contribute to observed high amount of m¹A in LC/MS analysis. Pyrosequencing and recently also deep sequencing methods of small non-coding RNAs in HIV-1 infected cells have proven the existence of a very abundant 18-nt tRNA fragment from tRNA^{Lys}_{TTT-3.1} that is complementary to the HIV-1 primer binding site^{42,43}. Rather than being a primer of reverse transcription, this tRNA fragment when overexpressed led to a decrease in viral replication. Nevertheless, the concentration of these tRNA fragments was so low that we were neither able to observe the fragments in isolated RNA from infected cells nor in packageomic RNA. Other types of 3' tRNA fragments were observed only in Northern blot analysis of fragmented RNA. Therefore, we also ruled out the possibility that m¹A can come from any type of tRNA fragments.

As the role of primer tRNA^{Lys}_{TTT-3.1} is quite well understood, the function of nonprimer tRNAs such as tRNA^{Lys}_{CTT-2.1}, tRNA^{Lys}_{CTT-1.1}, tRNA^{Asp}_{GTC-2.1} or tRNA^{Asn}_{GTT-2.1} is still very enigmatic. One of the hypothesis suggests that the matrix domain of the HIV-1 Gag protein binds almost exclusively to specific tRNAs in the cytosol⁴⁴. tRNAs shield the membrane-binding surface of matrix and regulate the interaction with intracellular membranes prior reaching the plasma membrane²⁷. Cellular tRNAs might also help to import HIV-1 intracellular reverse transcription complex to nucleus⁴⁵. Another theory suggests that the enrichment of particular tRNAs in virion can manipulate with tRNA pool in cells and enhance production of the Gag polyprotein and virus production in general⁴⁶. In any case, the importance of nonprimer tRNAs in virion is very high. In this work, we bring new tool – LC/MS in combination with deep sequencing – to study the virion RNA composition. Specific RNA modifications such as m¹A can bring us missing information layer and in future, we can calculate the RNA composition of other viruses. Moreover, these techniques can be used for studies of an impact of viral infection on various RNA modification in host transcriptome.

Methods

Cell culture, transfections and infections. The human CD4 + T-cell line MT4 (NIH AIDS Reagent Program, Division of AIDS, NIAID, NIH from Dr. Douglas Richman) and the human embryonic kidney HEK293T cell line (American Type Culture Collection, LGC Standards, UK) were cultured under standard conditions at 37 °C under a humidified (>90%) atmosphere of 5% CO₂/95% air. The MT4 cell line was cultured in RPMI 1640 w/o L-Glutamine and 25 mM Hepes supplemented with 10% FBS, penicillin (100 U/mL) and streptomycin (100 µg/mL) (all Sigma-Aldrich). The HEK293T cell line was cultured in DMEM high glucose supplemented with 10% FBS, penicillin (100 U/mL) and streptomycin (100 µg/mL) (all Sigma-Aldrich).

Isolation of large and small RNA fractions from the cell culture. MT4 cells were collected by centrifugation (225 × g, 5 min, and 20 °C), HEK293T cells were collected by trypsinization and subsequent centrifugation as above. Cells pellets were washed with PBS and cells were lysed with RNazol reagent (Sigma-Aldrich). Large and small RNA fractions were purified according to the RNazol manufacturer's protocol. The RNA concentration was determined on NanoDrop ONE (ThermoFisher Scientific) and the RNA sample quality control was performed on a 4200 TapeStation System (Agilent).

Infection. MT4 cells were initially infected with a cell-free HIV-1 strain NL4-3, which was generated by transient transfection of HEK293T cells with a pNL4-3 plasmid (obtained through NIH AIDS Reagent Program, Division of AIDS, NIAID, NIH from Dr. Malcolm Martin). The infected cultures were subsequently expanded by co-cultivation. 48 h post-infection, cell culture supernatants containing viral particles and infected cells were added to uninfected MT-4 cells (5×10^5 cells per mL) at a ratio of 1:9. The co-culture was synchronized by three successive additions of infected culture supernatant to uninfected MT4 cells (5×10^5 cells per mL, the ratio of 1:9, 27 h between infections).

Virus-containing supernatants were harvested 40 h after the last synchronization step, cleared by centrifugation ($225 \times g$, 5 min, 20°C) and filtration (0.45 μm pore size cellulose-acetate filter (VWR)), and stored at -80°C .

Infectious titres were determined as 50% tissue culture infectious dose by endpoint titration using serial 10-fold dilutions of the virus on TZM-bl cells⁴⁷.

Viral particles purification and RNA isolation. *Sucrose cushion isolation.* Virus particles were concentrated from cleared culture medium by centrifugation through a cushion of 20% (wt./wt.) sucrose in phosphate-buffered saline (PBS) ($90\,000 \times g$, 90 min, 4°C). The pellet was resuspended in RNase/DNase buffer (Tris HCl 100 mM, MgCl_2 25 mM, CaCl_2 25 mM) with DNase I (10 U/mL, New England BioLabs - NEB), RNase I (200 U/mL) and RNase A (20 mg/mL, both ThermoFisher Scientific) and incubated 2 h at 37°C . RNase/DNase treatment was stopped by adding RNazol (Sigma-Aldrich).

Mock medium was prepared in the same way from uninfected MT-4 cells.

OptiPrep gradient isolation. Virus particles were concentrated and cleared through a sucrose cushion as described above. The virus pellet was resuspended in PBS, loaded to the top of the iodixanol gradient (6% to 35% OptiPrep Density Gradient medium diluted in PBS, Sigma-Aldrich) and ultracentrifuged ($90\,000 \times g$, 90 min, 4°C). HIV-containing fractions were detected by western blot analysis using the anti-HIV capsid protein antibody. Selected fractions were collected, diluted with PBS five times and the virus was pelleted by ultracentrifugation ($90\,000 \times g$, 45 min, 4°C). The virus-containing pellet was resuspended in RNase/DNase buffer and RNase/DNase treatment was performed as described above.

Western blot analysis. Samples from each fraction of the Optiprep gradient were mixed with loading buffer in the ratio of 5:1 and denatured for 5 min at 95°C . Separation was carried out at 15% SDS PAGE at constant voltage 150 V for 90 min. Separated proteins were transferred to polyvinylidene difluoride (PVDF) membrane (Bio-Rad) and blocked at casein (Blocker Casein, ThermoFisher Scientific). HIV-1 CA protein was detected with polyclonal anti HIV-1 CA antibody (sera of rabbit immunized with purified HIV-1 CA protein, produced at Institute of Physiology CAS; dilution 1:1000, 1 h, RT) and as secondary antibody was used Goat anti Rabbit IgG labelled with horseradish peroxidase (1:10000, 1 h, RT, Sigma-Aldrich). After washing, the membranes were incubated with SuperSignal West Femto Maximum Sensitivity Substrate (ThermoFisher Scientific) and the intensity of chemiluminescence was detected using the CCD camera (Las-3000, software Image Reader Las-3000, Fujifilm) (Supplementary Figure S7).

RNA from viral particles was purified by Zymo-Spin™ IIC Columns (Direct-zol™ RNA MiniPrep Plus, Zymo) according to the manufacturer's protocol. The quality of RNA samples was checked by HS RNA ScreenTape. (Supplementary Figure S4) RNA samples were quantified by an RNA High Sensitivity Assay (Quibit 4 Fluorometer, ThermoFisher Scientific), and the presence of HIV gRNA was confirmed by RT-PCR (LightCycler, Roche) (Supplementary Figure S3).

RNA digestion and LC/MS analysis. RNA samples (1–4 μg) were fully digested by Nuclease P1 (1 U/ μg of RNA, Sigma-Aldrich) in 40 μL of 50 mM ammonium acetate buffer (pH 4.5) for 1 h at 37°C . After addition of Alkaline phosphatase (CIP, 1 U/ μg of RNA, NEB) and CutSmart buffer (final concentration $1 \times$, NEB), the samples were incubated for another 1 h at 37°C . Digested RNA samples were diluted in 200 μL and purified over Microcon® – 10 kDa centrifugal filters (Merck). The flow-through was concentrated using a SpeedVac system to the volume of 20 μL for LC-MS analysis.

All samples were measured in technical duplicates. The separation of the digested RNA samples (8 μL injection volume) was performed by an LC system (I-Class, Waters) on a C18 column (Acquity UPLC® BEH C18 1.7 μm , 15 cm, Waters) at 40°C using a gradient of water (A) and acetonitrile (B), each containing 0.1% (v/v) formic acid⁴⁸. The gradient was 0–6 min, 100% A; 6–7.5 min, 100–99% A; 7.5–9.5 min, 99–94% A; 9.5–15 min, 94% A; 15–25 min, 94–50% A; 25–27 min, 50–20%; 27–29.5 min, 20% A; 29.5–30 min, 20–100% A; 30–40 min, 100% A. The flow rate was 0.05 mL/min. The autosampler cooled the samples to 8°C . The LC system was coupled on-line to a mass spectrometer (Synapt G2, Waters) to acquire masses of nucleosides by electrospray ionisation. Ions were scanned in a positive polarity mode over full-scan range of m/z 100–1200. The source parameters were as follows: capillary voltage, 3 kV; source temperature, 150°C ; sampling cone, 40; extraction cone, 5; desolvation temperature, 450°C ; desolvation gas flow, 600 L/h.

All mass chromatograms were analysed employing the MassLynx V4.1 software. Mixtures of nucleoside standards ($m^1\text{A}$, $m^6\text{A}$, Am, A, $t^6\text{A}$; Jena Bioscience, Sigma-Aldrich, CarboSynth) at three different amounts: 64, 320 and 1600 fmol each were injected on a column to compare the response of each nucleoside under defined ionization conditions. Mixtures were measured in the technical triplicates. For each standard, an extracted ion chromatogram (EIC) was generated using a major fragment observed in its full scan spectrum (fragmentation occurs in the ion source). The chromatographic peaks in EICs were integrated. The standard peak area (area under the curve, AUC) was used to calculate the ionization efficiency ratio of the tested nucleosides in this concentration range (Supplementary Table S3, Figures S1, S2).

The chromatographic peaks of the major fragments in EICs were integrated. The AUC was used to calculate the percentage of the adenosine modifications (Fig. 1A,B).

Deep sequencing library preparation. Deep sequencing libraries were prepared using a combination of three protocols^{12,31,49}.

Chemical fragmentation (metal-ion induced) was used to achieve size distributions of the fragments from 50–200 nt. RNA samples (1–2 µg) were incubated with 100 mM ZnCl₂ in 100 mM Tris-HCl buffer at pH 7.4 at 75 °C for 1 min. The reaction was terminated by addition of EDTA at a final concentration of 50 mM. Samples were ethanol precipitated and the size of the RNA fragments was verified by HS RNA Screen Tape[®].

One half of each sample was incubated with alkaline buffer (50 mM Na₂CO₃, 2 mM EDTA, pH 10.4) for 1 h at 60 °C to convert m¹A into m⁶A via Dimroth rearrangement. Samples were purified by RNA Clean & Concentrator columns (Zymo) and analysed on HS RNA Screen Tape[®].

After denaturation of the RNA samples at 90 °C for 30 s, followed by cooling down on ice, dephosphorylation was performed by 0.5 U of FastAP alkaline phosphatase (ThermoFisher Scientific) in dephosphorylation buffer (at a final concentration 100 mM Tris-HCl, pH 7.4, 20 mM MgCl₂, 0.1 mg/mL BSA and 100 mM 2-mercaptoethanol) for 30 min at 37 °C. The whole procedure was repeated, followed by final heat deactivation of the enzyme at 75 °C for 5 min.

A pre-adenylated adaptor was prepared as described previously⁴⁹ (for the sequence see Supplementary Table S6). Ligation at the 3'-end of RNA was performed at 4 °C for 72 h in dephosphorylation buffer, containing in addition, 15% DMSO, 5 µM adenylated 3'-RNA adaptor, 0.5 U/µL T4 RNA ligase (ThermoFisher Scientific) and 1 U/µL T4 RNA ligase 2 truncated (NEB). The reaction was stopped by heating to 75 °C for 15 min. Unligated 3'-adaptor was removed by 5'-Deadenylase (NEB) and Lambda exonuclease (ThermoFisher Scientific). The mixture was ethanol precipitated.

Reverse transcription with SuperScript III (ThermoFisher Scientific, 10 U/µL) was performed in the First-Strand Buffer, containing RT primer (5 µM), dNTP mix (0.5 mM final conc.), DTT (5 mM), BSA (50 µg/µL) in 30 µL reaction mixture for 1 h at 50 °C. RT primer excess was digested by a combination of Lambda exonuclease, Exonuclease 1 and FastAP alkaline phosphatase (all ThermoFisher Scientific) after reaction. RNA was degraded by NaOH and samples were ethanol precipitated.

Reverse transcription with TGIRT[™]-III (InGex, 1 µL, 500 nM) was performed in 19 µL of reaction buffer (450 mM NaCl, 5 mM MgCl₂, 20 mM Tris-HCl, pH 7.5), with DTT (5 mM) and RT primer (5 µM) for 30 min at room temperature. After 30 min dNTPs (1.25 mM each, final volume 20 µL) were added and the reaction was incubated at 60 °C for 50 min. The reaction was stopped by the addition of 1 µL of 5 M NaOH and was incubated for 3 min at 95 °C. Samples were cooled down at room temperature, neutralized with 1 µL of 5 mM HCl and ethanol precipitated.

3'-Tailing of cDNA was performed using 1 U/µL of Deoxynucleotidyl transferase (TdT, ThermoFisher Scientific) in 1x TdT buffer containing 1.25 mM CTP for 30 min at 37 °C with heat deactivation (75 °C, 10 min). Double stranded DNA anchor was prepared as described previously⁴⁹. Ligation of dsDNA adaptor (1.25 µM) was done in 50 mM Tris-HCl buffer (pH 7.4), containing 10 µM ATP and 20 mM MgCl₂ with T4 DNA ligase (1.5 U/µL) at 4 °C for 72 h. The enzyme was heat deactivated at 65 °C for 10 min. Samples were ethanol precipitated and dissolved in 12 µL of water (molecular biology grade).

PCR amplification was performed with barcoded PCR primers (Supplementary Table S6) in 38 cycles in ThermoPol reaction buffer 1 × (NEB), with 5 µM of each barcoded primer, 0.5 mM dNTPs (each) and 0.25 U of *Taq* DNA Polymerase (NEB) in 20 µL of total reaction mixture. Initial denaturation was performed at 95 °C for 60 s, following by annealing for 60 s at 54 °C, elongation for 60 s at 68 °C and denaturation for 30 s at 95 °C. Final extension was performed at 68 °C for 5 min.

PCR reaction mixture was loaded on 1.3% agarose gel (140 V for 2 h). Fractions between 100–400 nt were cut and DNA was extracted from the gel by NucleoSpin[®] Gel and PCR Clean-up (Macherey –Nagel).

Bioinformatics. Libraries were trimmed using cutadapt⁵⁰ and Atropos⁵¹. Clean sequences longer than 20 bp were mapped to human genome and HIV-1 genome using bwa aligner v0.7.10-r789⁵². All statistics and graphs were generated by custom scripts (github:).

RNA detection by Northern blotting. Isolated RNA from HIV-1 particles and total RNA isolated from infected MT4 cells were each divided in two parts. One part was chemically fragmented as described for the deep sequencing libraries. Denaturing acrylamide gel (20%, 8 × 10 cm; 1 mm thickness) was prepared from 19:1 acrylamide:bis-acrylamide in 0.5x MOPS buffer (10x MOPS buffer stock containing 0.2 M MOPS pH 7.0, 50 mM NaOAc and 10 mM EDTA) and 7 M urea. The polymerized gel was pre-run at 100 V for 30 min in 0.5x MOPS buffer. 15 µL of the RNA samples (400–600 ng of RNA/sample, containing 7.3% formaldehyde, 50% formamide, 0.5x MOPS buffer and 0.01% bromphenol blue) were denatured for 15 min at 55 °C and loaded into the gel wells. The gel was initially run at 50 V for approximately 15 min to concentrate the samples in wells, and then at 150 V until the bromphenol blue reached 90% of the gel length. The gel was blotted onto a charged nylon membrane (Amersham Hybond-N +; GE Healthcare) by capillary transfer in 20x SSC buffer (3 M NaCl, 0.3 M tri-sodium citrate, pH adjusted to 7.0) overnight. The membrane was crosslinked twice on a default setting (120 mJ, 30 s) using electronic ultraviolet crosslinker (Ultralum). The crosslinked membrane was hybridized with 10 mL of Church buffer (70 mM NaH₂PO₄, 180 mM Na₂HPO₄, 7% SDS, 1% BSA, 1 mM EDTA, pH 7.2) at 45 °C for 1 h using a ProBlot hybridization oven (Labnet). Meanwhile, 5 µL of 100 µM probe (Sigma-Aldrich) was end-labelled using 20 U of T4 polynucleotide kinase (NEB), 2 µL of γ-³²P-ATP (3.3 µM, 10 µCi/µL; Hartmann analytic) in 20 µL of supplemented kinase buffer. The labelling was performed at 37 °C for 30 min. The enzyme was inactivated at 65 °C for 5 min and the probe was purified from unincorporated nucleotides using Micro Bio-Spin P-30

columns (BioRad) according to the manufacturer's instructions. The probe was added to the membrane in 10 mL of fresh Church buffer and hybridized at 45 °C overnight. The probe was washed twice for 10 min each with low stringency buffer (2x SSC + 0.1% SDS) and once with high stringency buffer (0.1x SSC + 0.1% SDS), all at 45 °C. The membrane was sealed in foil, incubated with phosphor imaging plate (GE healthcare) and read using Typhoon FLA 9500 (GE Healthcare).

Data Availability

Data from this manuscript is available upon request from the authors.

References

- Helm, M. & Alfonzo, J. D. Posttranscriptional RNA Modifications: Playing Metabolic Games in a Cell's Chemical Legoland. *Chemistry & Biology* **21**, 174–185, <https://doi.org/10.1016/j.chembiol.2013.10.015> (2014).
- Helm, M. & Motorin, Y. Detecting RNA modifications in the epitranscriptome: predict and validate. *Nature Reviews Genetics* **18**, 275, <https://doi.org/10.1038/nrg.2016.169> (2017).
- Carlile, T. M. *et al.* Pseudouridine profiling reveals regulated mRNA pseudouridylation in yeast and human cells. *Nature* **515**, 143, <https://doi.org/10.1038/nature13802>, <https://www.nature.com/articles/nature13802#supplementary-information> (2014).
- Schwartz, S. *et al.* Transcriptome-wide Mapping Reveals Widespread Dynamic-Regulated Pseudouridylation of ncRNA and mRNA. *Cell* **159**, 148–162, <https://doi.org/10.1016/j.cell.2014.08.028> (2014).
- Squires, J. E. *et al.* Widespread occurrence of 5-methylcytosine in human coding and non-coding RNA. *Nucleic Acids Research* **40**, 5023–5033, <https://doi.org/10.1093/nar/gks144> (2012).
- Sakurai, M., Yano, T., Kawabata, H., Ueda, H. & Suzuki, T. Inosine cyanoethylation identifies A-to-I RNA editing sites in the human transcriptome. *Nature Chemical Biology* **6**, 733, <https://doi.org/10.1038/nchembio.434>, <https://www.nature.com/articles/nchembio.434#supplementary-information> (2010).
- Cahová, H., Winz, M.-L., Höfer, K., Nübel, G. & Jäschke, A. NAD captureSeq indicates NAD as a bacterial cap for a subset of regulatory RNAs. *Nature* **519**, 374, <https://doi.org/10.1038/nature14020>, <https://www.nature.com/articles/nature14020#supplementary-information> (2014).
- Walters, R. W. *et al.* Identification of NAD⁺ capped mRNAs in *Saccharomyces cerevisiae*. *Proc. Natl. Acad. Sci. USA* **114**, 480–485, <https://doi.org/10.1073/pnas.1619369114> (2017).
- Jiao, X. *et al.* 5' End Nicotinamide Adenine Dinucleotide Cap in Human Cells Promotes RNA Decay through DXO-Mediated deNADding. *Cell* **168**, 1015–1027, <https://doi.org/10.1016/j.cell.2017.02.019> (2017).
- Dominissini, D. *et al.* Topology of the human and mouse m6A RNA methylomes revealed by m6A-seq. *Nature* **485**, 201, <https://doi.org/10.1038/nature11112>, <https://www.nature.com/articles/nature11112#supplementary-information> (2012).
- Meyer, K. D. *et al.* Comprehensive Analysis of mRNA Methylation Reveals Enrichment in 3' UTRs and near Stop Codons. *Cell* **149**, 1635–1646, <https://doi.org/10.1016/j.cell.2012.05.003> (2012).
- Dominissini, D. *et al.* The dynamic N1-methyladenosine methylome in eukaryotic messenger RNA. *Nature* **530**, 441, <https://doi.org/10.1038/nature16998>, <https://www.nature.com/articles/nature16998#supplementary-information> (2016).
- Zhang, C., Jia, G. & Reversible, R. N. A. Modification N1-methyladenosine (m1A) in mRNA and tRNA. *Genomics, Proteomics & Bioinformatics* **16**, 155–161, <https://doi.org/10.1016/j.gpb.2018.03.003> (2018).
- Safra, M. *et al.* The m1A landscape on cytosolic and mitochondrial mRNA at single-base resolution. *Nature* **551**, 251, <https://doi.org/10.1038/nature24456>, <https://www.nature.com/articles/nature24456#supplementary-information> (2017).
- Gokhale, N. S. *et al.* N6-Methyladenosine in Flaviviridae Viral RNA Genomes Regulates Infection. *Cell Host & Microbe* **20**, 654–665, <https://doi.org/10.1016/j.chom.2016.09.015> (2016).
- Kennedy, E. M. *et al.* Posttranscriptional m6A Editing of HIV-1 mRNAs Enhances Viral Gene Expression. *Cell Host & Microbe* **19**, 675–685, <https://doi.org/10.1016/j.chom.2016.04.002> (2016).
- Keene, S. E., King, S. R. & Telesnitsky, A. 7SL RNA Is Retained in HIV-1 Minimal Virus-Like Particles as an S-Domain Fragment. *Journal of Virology* **84**, 9070–9077, <https://doi.org/10.1128/jvi.00714-10> (2010).
- Telesnitsky, A. & Wolin, S. The Host RNAs in Retroviral Particles. *Viruses* **8**, 235 (2016).
- Larsen, K. P. *et al.* Architecture of an HIV-1 reverse transcriptase initiation complex. *Nature* **557**, 118–122, <https://doi.org/10.1038/s41586-018-0055-9> (2018).
- Zhang, Z., Yu, Q., Kang, S.-M., Buescher, J. & Morrow, C. D. Preferential Completion of Human Immunodeficiency Virus Type 1 Proviruses Initiated with tRNA³ Lys rather than tRNA^{1,2} Lys. *Journal of Virology* **72**, 5464–5471 (1998).
- Auxilien, S., Keith, G., Le Grice, S. F. J. & Darlix, J.-L. Role of Post-transcriptional Modifications of Primer tRNA^{Lys,3} in the Fidelity and Efficacy of Plus Strand DNA Transfer during HIV-1 Reverse Transcription. *Journal of Biological Chemistry* **274**, 4412–4420, <https://doi.org/10.1074/jbc.274.7.4412> (1999).
- Kleiman, L., Jones, C. P. & Musier-Forsyth, K. Formation of the tRNA^{Lys} packaging complex in HIV-1. *FEBS Letters* **584**, 359–365, <https://doi.org/10.1016/j.febslet.2009.11.038> (2010).
- Bilbille, Y. *et al.* The structure of the human tRNA^{Lys3} anticodon bound to the HIV genome is stabilized by modified nucleosides and adjacent mismatch base pairs. *Nucleic Acids Research* **37**, 3342–3353, <https://doi.org/10.1093/nar/gkp187> (2009).
- Eckwahl, M. J. *et al.* Analysis of the human immunodeficiency virus-1 RNA packageome. *RNA*. <https://doi.org/10.1261/rna.057299.116> (2016).
- Eckwahl, M. J., Sim, S., Smith, D., Telesnitsky, A. & Wolin, S. L. A retrovirus packages nascent host noncoding RNAs from a novel surveillance pathway. *Genes & Development* **29**, 646–657, <https://doi.org/10.1101/gad.258731.115> (2015).
- Schopman, N. C. T. *et al.* Selective packaging of cellular miRNAs in HIV-1 particles. *Virus Research* **169**, 438–447, <https://doi.org/10.1016/j.virusres.2012.06.017> (2012).
- Eckwahl, M. J., Telesnitsky, A. & Wolin, S. L. Host RNA Packaging by Retroviruses: A Newly Synthesized Story. *mBio* **7**, <https://doi.org/10.1128/mBio.02025-15> (2016).
- Berkowitz, R., Fisher, J. & Goff, S. P. In *Morphogenesis and Maturation of Retroviruses* (ed Hans-Georg Kräusslich) 177–218 (Springer Berlin Heidelberg, 1996).
- Bagiński, B. *et al.* MODOMICS: a database of RNA modification pathways. 2017 update. *Nucleic Acids Research* **46**, D303–D307, <https://doi.org/10.1093/nar/gkx1030> (2017).
- Hauenschild, R. *et al.* The reverse transcription signature of N1-methyladenosine in RNA-Seq is sequence dependent. *Nucleic Acids Research* **43**, 9950–9964, <https://doi.org/10.1093/nar/gkv895> (2015).
- Tserovski, L. *et al.* High-throughput sequencing for 1-methyladenosine (m1A) mapping in RNA. *Methods* **107**, 110–121, <https://doi.org/10.1016/j.jymeth.2016.02.012> (2016).
- Kietrys, A. M., Velema, W. A. & Kool, E. T. Fingerprints of Modified RNA Bases from Deep Sequencing Profiles. *Journal of the American Chemical Society* **139**, 17074–17081, <https://doi.org/10.1021/jacs.7b07914> (2017).
- Oerum, S., Dégut, C., Barraud, P. & Tisné, C. m1A Post-Transcriptional Modification in tRNAs. *Biomolecules* **7**, 20 (2017).
- Roovers, M. *et al.* A primordial RNA modification enzyme: the case of tRNA (m1A) methyltransferase. *Nucleic Acids Research* **32**, 465–476, <https://doi.org/10.1093/nar/gkh191> (2004).

35. Narayanan, A. *et al.* Exosomes Derived from HIV-1-infected Cells Contain Trans-activation Response Element RNA. *Journal of Biological Chemistry* **288**, 20014–20033, <https://doi.org/10.1074/jbc.M112.438895> (2013).
36. Wei, F.-Y. *et al.* Deficit of tRNA^{Lys} modification by Cdk11 causes the development of type 2 diabetes in mice. *The Journal of Clinical Investigation* **121**, 3598–3608, <https://doi.org/10.1172/JCI58056> (2011).
37. Jiang, M. *et al.* Identification of tRNAs incorporated into wild-type and mutant human immunodeficiency virus type 1. *Journal of Virology* **67**, 3246–3253 (1993).
38. Mak, J. *et al.* Role of Pr160gag-pol in mediating the selective incorporation of tRNA(Lys) into human immunodeficiency virus type 1 particles. *Journal of Virology* **68**, 2065–2072 (1994).
39. Pavon-Eternod, M., Wei, M., Pan, T. & Kleiman, L. Profiling non-lysyl tRNAs in HIV-1. *RNA* **16**, 267–273, <https://doi.org/10.1261/rna.1928110> (2010).
40. Onafuwa-Nuga, A. A., Telesnitsky, A. & King, S. R. 7SL RNA, but not the 54-kd signal recognition particle protein, is an abundant component of both infectious HIV-1 and minimal virus-like particles. *RNA* **12**, 542–546, <https://doi.org/10.1261/rna.2306306> (2006).
41. McIntyre, W. *et al.* Positive-sense RNA viruses reveal the complexity and dynamics of the cellular and viral epitranscriptomes during infection. *Nucleic Acids Research* **46**, 5776–5791, <https://doi.org/10.1093/nar/gky029> (2018).
42. Yeung, M. L. *et al.* Pyrosequencing of small non-coding RNAs in HIV-1 infected cells: evidence for the processing of a viral-cellular double-stranded RNA hybrid. *Nucleic Acids Research* **37**, 6575–6586, <https://doi.org/10.1093/nar/gkp707> (2009).
43. Schopman, N. C. T. *et al.* Deep sequencing of virus-infected cells reveals HIV-encoded small RNAs. *Nucleic Acids Research* **40**, 414–427, <https://doi.org/10.1093/nar/gkr719> (2012).
44. Kutluay, S. B. *et al.* Global Changes in the RNA Binding Specificity of HIV-1 Gag Regulate Virion Genesis. *Cell* **159**, 1096–1109, <https://doi.org/10.1016/j.cell.2014.09.057> (2014).
45. Zaitseva, L., Myers, R. & Fassati, A. tRNAs Promote Nuclear Import of HIV-1 Intracellular Reverse Transcription Complexes. *PLOS Biology* **4**, e332, <https://doi.org/10.1371/journal.pbio.0040332> (2006).
46. Li, M. *et al.* Codon-usage-based inhibition of HIV protein synthesis by human schlafen 11. *Nature* **491**, 125, <https://doi.org/10.1038/nature11433>, <https://www.nature.com/articles/nature11433#supplementary-information> (2012).
47. Reed, L. J. & Muench, H. A simple method of estimating fifty per cent endpoints¹². *American Journal of Epidemiology* **27**, 493–497, <https://doi.org/10.1093/oxfordjournals.aje.a118408> (1938).
48. Su, D. *et al.* Quantitative analysis of ribonucleoside modifications in tRNA by HPLC-coupled mass spectrometry. *Nature Protocols* **9**, 828, <https://doi.org/10.1038/nprot.2014.047> (2014).
49. Winz, M.-L. *et al.* Capture and sequencing of NAD-capped RNA sequences with NAD captureSeq. *Nature Protocols* **12**, 122, <https://doi.org/10.1038/nprot.2016.163>, <https://www.nature.com/articles/nprot.2016.163#supplementary-information> (2016).
50. Martin, M. Cutadapt removes adapter sequences from high-throughput sequencing reads. *2011* **17**, 3, <https://doi.org/10.14806/ej.17.1.200> (2011).
51. Didion, J. P., Martin, M. & Collins, F. S. Atropos: specific, sensitive, and speedy trimming of sequencing reads. *PeerJ* **5**, e3720, <https://doi.org/10.7717/peerj.3720> (2017).
52. Li, H. & Durbin, R. Fast and accurate short read alignment with Burrows–Wheeler transform. *Bioinformatics* **25**, 1754–1760, <https://doi.org/10.1093/bioinformatics/btp324> (2009).

Acknowledgements

We are grateful to Dr. J. Kozák for radioactive labelling of probes for northern blot analysis. This work was supported by the Ministry of Education, Youth and Sports (Czech Republic), programme ERC CZ (LL1603). Funding for open access charge: Ministry of Education, Youth and Sports. The bioinformatics part of the work including access to computing and storage facilities was supported by the ELIXIR CZ research infrastructure project (MEYS Grant No: LM2015047).

Author Contributions

A.S. and H.C. conceived the study. A.S., M.H., M.P., J.H. and H.C. designed the experiments. A.S., B.S., J.T. and M.Z. performed the experiments. J.W., J.C., J.P. and H.C. supervised the work. O.M. and J.P. analysed bioinformatics data. A.S., B.S., J.T. and H.C. wrote the paper.

Additional Information

Supplementary information accompanies this paper at <https://doi.org/10.1038/s41598-019-45079-1>.

Competing Interests: The authors declare no competing interests.

Publisher's note: Springer Nature remains neutral with regard to jurisdictional claims in published maps and institutional affiliations.



Open Access This article is licensed under a Creative Commons Attribution 4.0 International License, which permits use, sharing, adaptation, distribution and reproduction in any medium or format, as long as you give appropriate credit to the original author(s) and the source, provide a link to the Creative Commons license, and indicate if changes were made. The images or other third party material in this article are included in the article's Creative Commons license, unless indicated otherwise in a credit line to the material. If material is not included in the article's Creative Commons license and your intended use is not permitted by statutory regulation or exceeds the permitted use, you will need to obtain permission directly from the copyright holder. To view a copy of this license, visit <http://creativecommons.org/licenses/by/4.0/>.

© The Author(s) 2019



Honeybee Iflaviruses Pack Specific tRNA Fragments from Host Cells in Their Virions

Anna Šimonová,^[a, b] Veronika Romanská,^[a] Barbora Benoni,^[a, b] Karel Škubník,^[c]
Lenka Šmerdová,^[c] Michaela Procházková,^[c] Kristina Spustová,^[a] Ondřej Moravčík,^[d]
Lenka Gahurova,^[a, e] Jan Pačes,^[d, f] Pavel Plevka,^[c] and Hana Cahová*^[a]

The *Picornavirales* include viruses that infect vertebrates, insects, and plants. It was believed that they pack only their genomic mRNA in the particles; thus, we envisaged these viruses as excellent model systems for studies of mRNA modifications. We used LC–MS to analyze digested RNA isolated from particles of the sacbrood and deformed wing iflaviruses as well as of the echovirus 18 and rhinovirus 2 picornaviruses. Whereas in the picornavirus RNAs we detected only *N*⁶-methyladenosine and 2'-*O*-methylated nucleosides, the iflavirus RNAs contained a

wide range of methylated nucleosides, such as 1-methyladenosine (*m*¹A) and 5-methylcytidine (*m*⁵C). Mapping of *m*¹A and *m*⁵C through RNA sequencing of the SBV and DWV RNAs revealed the presence of tRNA molecules. Both modifications were detected only in tRNA. Further analysis revealed that tRNAs are present in form of 3' and 5' fragments and they are packed selectively. Moreover, these tRNAs are typically packed by other viruses.

Introduction

More than 170 RNA modifications are currently known to be naturally present in various types of RNA.^[1] They are the best studied in the abundant RNA moieties such as tRNA and rRNA. The discovery of the *N*⁶-methyladenosine (*m*⁶A) in mRNA^[2] represents a milestone in the field and triggered a new search for other modifications in coding RNA such as mRNA or viral genomic RNA. The detection of RNA modifications in mRNA is

still limited by the amount and purity of the mRNA. The contamination of mRNA by tRNA and rRNA causes false positive LC–MS detection of RNA modifications coming from these abundant RNA species. Alternative detection techniques selective to particular RNA modification are combined with RNA sequencing (RNA-seq) and bring information on exact position of the modification in the RNA sequence. Nevertheless, some methods suffer from false positive output as well. Typical example is interaction of modification specific antibodies with unmodified parts of RNA.^[3] Another example can be false positive detection of *m*⁵C in highly structured RNA such as viroids.^[4] Therefore, it is necessary to combine various techniques to prove the presence of certain RNA modifications in low abundant species.^[5] While *m*⁶A is an indisputable marker on coding RNA with significant impact on RNA stability and recognition proteins as the writers, erasers and readers are known, the roles and mechanisms of action for other RNA modifications should be still revealed. So far, only *m*⁶A, *m*⁵C, Inosine (I) and 2'-*O*-methyl (Nm) were discovered and confirmed as part of various viral genomic or viral encoded mRNA.^[6]

In our search for viral mRNA modifications, we focused on various representatives from insect and human *Picornavirales* (sacbrood virus (SBV), deformed wing virus (DWV), human rhinovirus-2 (RV2) and Echovirus 18 (E18)) as model systems to reveal RNA modifications in their genomic RNA. Until now, only *m*⁶A was reported to be present in RNA from picornavirus enterovirus 71.^[7] It was shown that the presence of *m*⁶A in two positions of genomic viral RNA positively modulated viral replication.

The family *Picornaviridae* includes viruses that infect vertebrates and cause numerous diseases in humans. The illnesses caused by picornaviruses range from mild upper and lower respiratory tract infections, gastroenteritis, hepatitis, hand-foot-and-mouth-disease to life-threatening encephalitis.^[8] Human rhinoviruses, including rhinovirus 2 (RV2) are responsible

[a] A. Šimonová, V. Romanská, B. Benoni, K. Spustová, Dr. L. Gahurova, Dr. H. Cahová
Institute of Organic Chemistry and Biochemistry of the Czech Academy of Sciences
Flemingovo nam. 2, 16610 Prague 6 (Czech Republic)
E-mail: cahova@uochb.cas.cz

[b] A. Šimonová, B. Benoni
First Faculty of Medicine Charles University
Katerinská 32, 12108 Prague 2 (Czech Republic)

[c] Dr. K. Škubník, Dr. L. Šmerdová, M. Procházková, Dr. P. Plevka
Structural Virology, Central European Institute of Technology
Masaryk University, Kamenice 753/5, 62500 Brno (Czech Republic)

[d] O. Moravčík, Dr. J. Pačes
Institute of Molecular Genetics of the Czech Academy of Sciences
14220 Prague (Czech Republic)

[e] Dr. L. Gahurova
Department of Molecular Biology and Genetics
Faculty of Science, University of South Bohemia
Branisovska 1760, 37005 České Budějovice (Czech Republic)

[f] Dr. J. Pačes
University of Chemistry and Technology
16628 Prague (Czech Republic)

Supporting information for this article is available on the WWW under <https://doi.org/10.1002/cbic.202200281>

This article is part of the Special Collection ChemBioTalents2022. Please see our homepage for more articles in the collection.

© 2022 The Authors. ChemBioChem published by Wiley-VCH GmbH. This is an open access article under the terms of the Creative Commons Attribution Non-Commercial License, which permits use, distribution and reproduction in any medium, provided the original work is properly cited and is not used for commercial purposes.

for 40% of the common cold cases that result in yearly cost of about \$16 billion in treatments and lost working hours within the United States alone.^[8] Echovirus 18, an enterovirus from the family *Picornaviridae*, causes aseptic meningitis and exanthema in humans.^[9]

Apart from human viruses, the most important honeybee viruses also belong to the order *Picornavirales*, particularly the family *Iflaviridae*: deformed wing virus (DWV) and sacbrood virus (SBV).^[10] Honeybee (*Apis mellifera*) is found all over the world and plays a vital role in agricultural industry by providing pollination services for many food crops. However, the virus infections are one of the major threats to the health and productivity of the honeybee colonies.^[11]

For our study, we selected *Picornavirales* as their RNA serves as both the genomic and mRNA and their virions should contain only viral RNA. Therefore, the RNA purified from the particle should not be contaminated by the otherwise abundant host tRNA and rRNA,^[12] as it is common for cellular mRNA or for viral RNA isolated from retroviruses such as HIV-1.^[13] Thus, this work should answer the basic question: what are the typical RNA modifications in mRNA.

In this work, we isolated RNA from pure virions and we digested it into form of nucleosides. The digested mixtures were then analyzed using LC–MS and compared with standard modified nucleosides. While we observed only 2'-O-methylated nucleosides in RNA isolated from human picornaviruses (RV2, E18), the RNA isolated from insect viruses (SBV and DWV) contained significant amount of other methylated nucleosides e.g. 1-methyladenosine (m¹A) or m⁵C. Therefore, we applied two profiling techniques in combination with RNA-seq to map m¹A and m⁵C in the viral RNA isolated from iflaviruses. The bioinformatic analysis of these RNA-seq libraries did not confirm m¹A and m⁵C in the viral genomic RNA. Nevertheless, we detected specific honeybee tRNAs,^[14] which were co-packed in the virions together with viral genomic RNA. Surprisingly, we observed only specific tRNAs such as various isoforms of tRNA^{LysTTT}, tRNA^{LysCTT}, tRNA^{GlyGCC} or tRNA^{AspGTC}. We compared this finding with a codon usage of the host organism – honeybee. With exception of Lys AAA codon, other do not belong among the most used tRNAs in the host organism. Moreover, these particular types of tRNA are also the most abundant in HIV-1 virions,^[13a–c] what suggests their general role in virus life cycle.



Hana received her PhD at UCT Prague and IOCB Prague in organic chemistry under the supervision of Prof. Michal Hocek. In 2011, she was awarded the Humboldt Research Fellowship and she joined Prof. Andres Jäschke's laboratory at Heidelberg University. As postdoctoral fellow, she worked on photo-switchable DNA and she developed NAD captureSeq for identification of NAD-RNA. She has been the head of the Junior Research Group of Chemical Biology at IOCB Prague since 2016. Together with her team she focuses on understanding the role of RNA modifications in viruses and other model organisms.

Nevertheless, the Northern blot analysis showed the presence of 3' and 5' tRNA fragments with length around 20 nt in viral particles, while the whole tRNAs were observed only in bee RNA.

Results

LC–MS analysis of RNA from virions

Virions of E18, RV2, SBV, and DWV were purified using CsCl gradient. The purity of the virions was confirmed using cryo-electron micrographs. Before RNA isolation from viral particles, any unpacked RNA or DNA was digested by RNase and DNase treatment (Figure S11). In the next step, the isolated RNA was digested by Nuclease P1 and Alkaline phosphatase into form of nucleosides and analyzed by LC–MS method (Figure 1a, Figure S12). The LC–MS analyses of the digested RNA from insect SBV, DWV and human RV2 and E18 were compared with common methylated nucleoside standards (1-methyladenosine (m¹A), N⁶-methyladenosine (m⁶A), 2'-O-methyladenosine (Am), 1-methylguanosine (m¹G), 2-methylguanosine (m²G), N⁷-methylguanosine (m⁷G), 2'-O-methylguanosine (Gm), 3-methylcytidine (m³C), 5-methylcytidine (m⁵C), 2'-O-methylcytidine (Cm), 5-methyluridine (m⁵U) and 2'-O-methyluridine (Um)) (Table S1, Figure S13, 4). The 2'-O-methylated nucleosides are known to be present in mRNA in general^[15] and we identified them almost in all samples. Also, the detection of m⁶A in viral RNA was expected.^[7] While human viruses did not contain any significant numbers of other methylated nucleotides, surprisingly, we identified substantial amount of various methylated nucleosides (m¹A, m¹G, m²G, m⁷G, m⁵C etc.) rather typical for tRNAs in RNA isolated from iflaviruses (Figure 1b, Figures S15–8).

RNA-seq for RNA modifications detection

The detected methylated nucleosides can come either from viral genomic RNA or from co-packed host RNA. Even though the co-packing of host RNA in the *Picornavirales* virions has not been reported yet, we also considered this option. To answer this question, we prepared RNA sequencing (RNA-seq) libraries with focus on m¹A (SBV) and m⁵C (SBV, DWV) profiling. The m¹A modification was detected by the method used recently for identification of m¹A positions in the RNA of HIV-1 viral particle.^[13a] As m¹A disturbs Watson-Crick base-pairing, it causes problems to reverse transcriptase in recognition and thus misincorporation or breaks can be observed in bioinformatic data. As a control we converted m¹A to m⁶A by Dimroth rearrangement (alkali conditions) (Figure 2a). We used two types of reverse transcriptases (Superscript III, TGIRT) for m¹A position confirmation.^[16] The m¹A position was then bioinformatically detected by misincorporation pattern (less prominent in the control samples after alkaline treatment). The m⁵C was detected by optimized bisulfite sequencing method (Figure 2a).

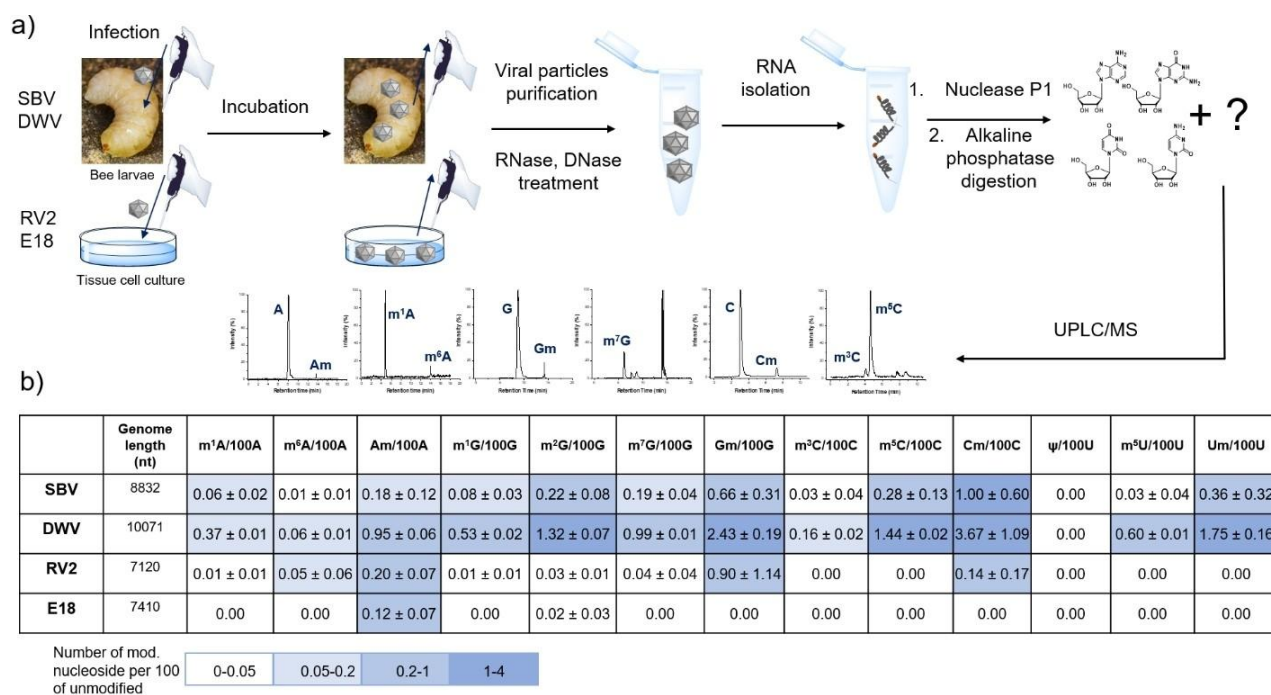


Figure 1. LC-MS analysis of RNA isolated from virions of insects Iflaviruses (SBV, DWV) and human Picornaviruses (RV2, E18). a) Scheme of workflow. b) Table with detected modified nucleosides per 100 unmodified for every virus. The shade of blue indicates the amount of detected methylated nucleoside.

The bioinformatic analysis revealed the presence of various types of host tRNA in the RNA isolated from virions of SBV and DWV. Surprisingly, the detected tRNAs correspond only partially to those, used by host organism the most. We identified mainly three types of tRNAs: tRNA^{GlyGCC-1}, tRNA^{AspGTC} and tRNA^{LysTTT} in both viruses and also tRNA^{LysCTT} in SBV (Figure 2b, c) and tRNA^{GluCTC} in DWV. Apart from these four tRNAs also other types were present in both viruses (Table SI 2). The m¹A profiling technique allowed us to confirm m¹A in some of the detected tRNAs e.g. in position 59 of tRNA^{LysCTT} and position 56 of tRNA^{GlyGCC-1} (Figures SI 9, 10). The disappearance of the base misincorporation (A for T) after alkali treatment was detected in experiments with both or at least one reverse transcriptase. Even though, we detected the misincorporations (base mismatch) of A in other tRNAs in otherwise typical positions for m¹A (8 and 10 in tRNA^{AspGTC} or 59 tRNA^{LysTTT}), we did not observe the disappearance of the signal after alkali treatment (Figures SI 10, 11). Thus, we concluded that other types of modifications must be present in these positions. The searching for this pattern (base mismatch at A position and disappearance after alkali treatment) in the genomic RNA of SBV did not convincingly show the presence of m¹A in SBV genomic RNA (Table SI 8, Figure SI 13).

The bisulfite sequencing confirmed the presence of various tRNAs in the RNA isolated from virions of SBV and DWV as well. 5-methylcytidine was detected through bisulfite sequencing in some of the most abundant tRNAs co-packed by SBV such as tRNA^{AspGTC} or co-packed by DWV tRNA^{AspGTC}, tRNA^{LysTTT} and tRNA^{GluCTC} (Tables SI 3, 4). 5-methylcytidine was usually observed in specific positions in 100% of reads of these tRNAs. Even

though, we observed partial conversion of some C to U in genomic RNA from samples treated by bisulfite, we presume that this is caused rather by incomplete bisulfite reaction than by the presence of m⁵C in these positions (Table SI 5, 6). Only around 6–7% of C in the particular positions were not converted to U.

Both sequencing experiments lead us to conclusion that m¹A, m⁵C and other methylated nucleotides come from the co-packed tRNAs. To support this hypothesis, we also searched for three types of modified adenosines that are typical for eukaryotic tRNAs in general:^[17] N⁶-threonylcarbamoyladenosine (t⁶A), 2-methylthio-N⁶-threonylcarbamoyladenosine (mS²t⁶A) and N⁶-isopentenyladenosine (i⁶A). These modifications are usually present close to anticodon loop and cause the reverse transcription falling i.e. coverage drop in RNA-seq data. The coverage drops were observed for all the detected tRNAs (Figures SI 9–12). In our LC-MS analysis of digested RNA isolated from virions, we compared our samples with LC-MS properties (detected mass and retention time) of standard t⁶A and with calculated mass of second two nucleosides (mS²t⁶A and i⁶A). We indeed observed these modified nucleosides in RNA isolated from SBV and DWV virions and not in human representative of *Picornavirales* RV2 and E18 (Table SI 7). This observation again confirms our finding that insects *Picornavirales* co-pack specific tRNAs in their virions, while two studied human viruses do not.

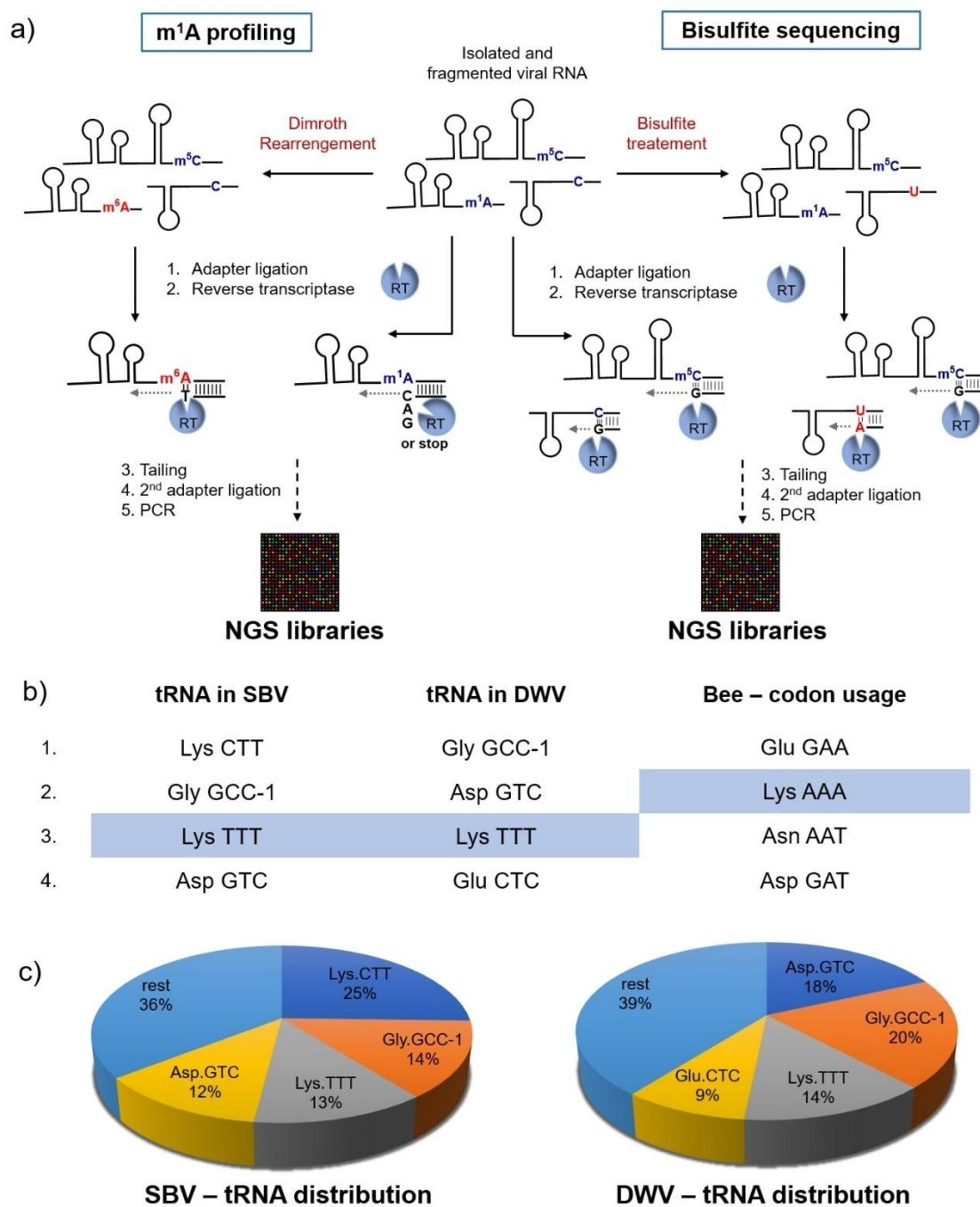


Figure 2. Detection of m¹A and m⁵C position in RNA isolated from virions. a) Scheme of m¹A profiling and bisulfite sequencing applied on isolated RNA. b) Table of the detected tRNAs in SBV, DWV and honeybee codon usage. The blue color represents the tRNA that is also among the most used one in host organism. c) The ratio of co-packed tRNAs in SBV (detected in 6 samples) and DWV (detected in 2 samples).

Northern blot analysis of RNA from virions

We also analyzed RNA isolated from honeybee pupae and from SBV and DWV by Northern blots with ³²P labeled probes for 3' and 5' ends and for central region of tRNA^{GlyGCC-1}, tRNA^{AspGTC}, tRNA^{LysTTT}, tRNA^{LysCTT} and tRNA^{GluCTC}. Surprisingly, we observed full length tRNAs in honeybee RNA but not in RNA from both viruses. Viruses contained only short fragments of these tRNAs.

We prepared RNA ladder with tRNA^{LysTTT} sequence of various size (21, 38 and 75 nt). The size of 3' end fragments is around 38 nt. We were not able to detect 5' end tRNA fragment of tRNA^{AspGTC} but other 5' tRNA fragments from tRNA^{GlyGCC-1}, tRNA^{LysTTT}, tRNA^{LysCTT} and tRNA^{GluCTC} were observed (Figure 3a, b). The size of the 5' end tRNA fragments is comparable or shorter than 3' tRNA fragments (Figure 3c). As we did not observe such tRNA fragments in the host organism, viruses probably trigger

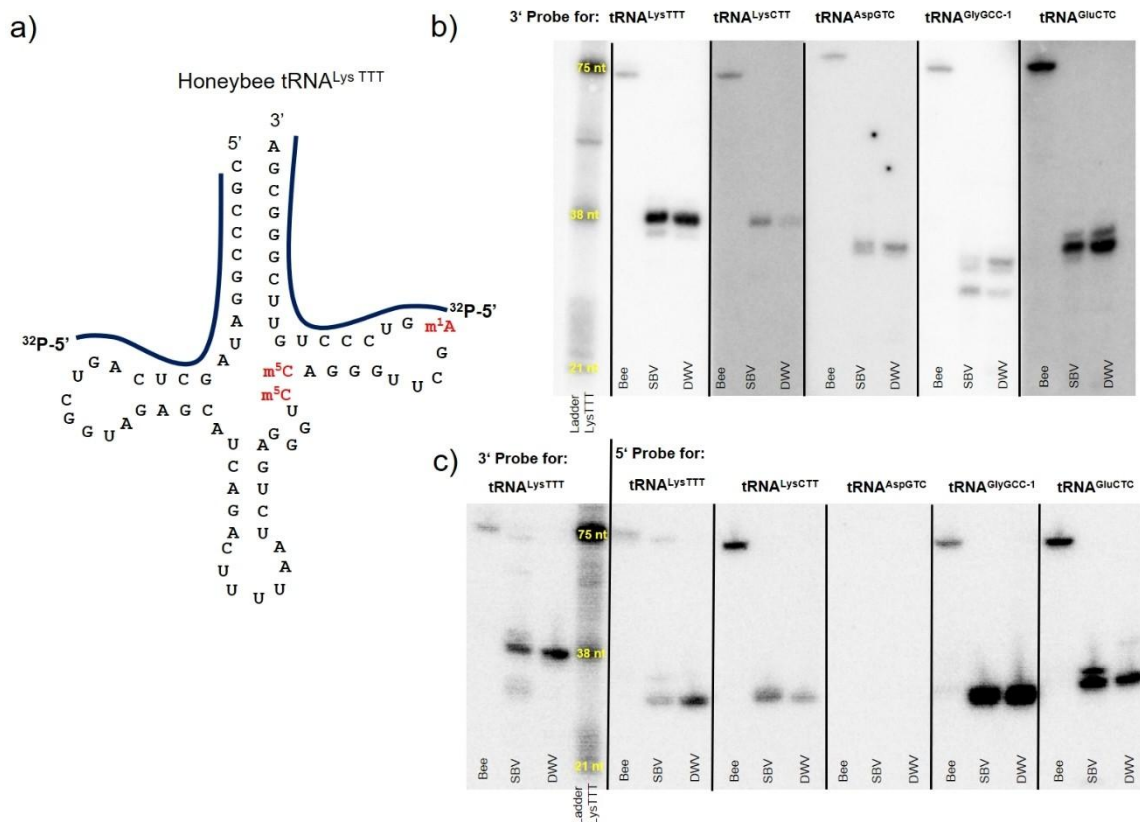


Figure 3. Detection of tRNAs in RNA isolated from Honeybee, SBV and DWV. a) Structure of Honeybee tRNA^{Lys}TTT. b) Northern blot analysis of isolated RNA and in vitro prepared RNA ladder with ³²P labeled probes for 3' end of tRNA^{Lys}TTT, tRNA^{Lys}CTT, tRNA^{Asp}GTC, tRNA^{Gly}GCC-1 and tRNA^{Glu}CTC. c) Northern blot analysis of isolated RNA and in vitro prepared RNA ladder with ³²P labeled probes for 3' end of tRNA^{Lys}TTT and 5' end of tRNA^{Lys}TTT, tRNA^{Lys}CTT, tRNA^{Asp}GTC, tRNA^{Gly}GCC-1 and tRNA^{Glu}CTC. (Experiments were performed in triplicate).

the formation of these tRNA fragments and/or selectively co-pack these tRNA fragments in their particles.

Discussion

The current pandemic teaches us that the viruses represent the major threat to human populations and that we do not have available any general antiviral useful in such situation. As we cannot presume, what other type of virus can threaten our society in future, it is necessary to learn as much as possible about virions composition and virus life cycle, in general.

Recently established epitranscriptomic field^[18] focuses on mRNA modifications. The major challenge in the identification of new RNA modifications lies in the purification of cellular mRNA. Usually the most abundant tRNAs and rRNAs contaminate mRNA and their typical RNA modifications can be misinterpreted as originating from mRNA. In our search for new types of mRNA modifications, we identified viruses from *Picornavirales* order as the most suitable model systems. Until now, it was believed that the virions of these viruses contain solely genomic RNA, which they also use as mRNA. Therefore, the RNA purified from virions of *Picornavirales* should not contain any cellular RNA contamination. As RNA modifications

help to virus to avoid the innate immune response of host organism and stabilize the viral RNA,^[6] we presumed that discovery of some new RNA modifications in genomic RNA from *Picornavirales*, would help us to understand better virus life cycle. For our study, we choose four representatives from the *Picornavirales* order: insect iflaviridae (SBV and DWV) and human picornaviridae (E18 and RV2). We isolated RNA from pure virions and digested it into form of nucleosides. The mixtures of nucleosides were analyzed by LC-MS and compared with external standards of nucleosides. Surprisingly, we observed wide range of methylated nucleosides in the RNA isolated from SBV and DWV. The human viruses contained only low amount of 2'-O-methylated nucleosides and m⁶A, which was recently detected also in enterovirus 71.^[7]

To determine the exact position of m¹A and m⁵C in viral RNA, we prepared RNA-seq libraries mapping m¹A and m⁵C (bisulfite sequencing). To our surprise, we identified certain types of tRNAs in both viral samples. We were also able to identify the exact positions of m¹A in and m⁵C in these co-packed tRNAs. The presence of these modifications was not conclusively confirmed in viral genomic RNA by our methods. This suggests that all the detected RNA modifications rather come from co-packed tRNAs. Moreover, in the light of the recent findings that e.g. m¹A is not present in human mRNA,^[19]

our findings confirms the latest theories that mRNA is not so heavily modified as it was expected. Thus the viral genomic and mRNA will not contain wide range of modifications.^[6] As we observed significant drops in tRNA reads (RNA-seq data), which are usually caused by sterically demanding modifications in close proximity of anticodon loop, we searched for three types of A modifications: t⁶A, mS²t⁶A and i⁶A, by LC-MS analysis. We confirmed the presence of all three modifications in RNA isolated from both viruses. This finding again confirms our theory that majority of detected modifications come from the co-packed tRNAs.

We also compared the types of co-packed tRNAs with codon-usage of honeybees to see whether these tRNAs that are the most abundant in host organism are also statistically co-packed in viral particle. Remarkably, the co-packed tRNAs do not correspond to ones most used by the host organism with only one exception – tRNA^{LysTTT}. In RNA isolate from virions from SBV, we identified four types of tRNAs: tRNA^{LysCTT}, tRNA^{GlyGCC-1}, tRNA^{LysTTT} and tRNA^{AspGTC} and from DWV, we identified beside tRNA^{GlyGCC-1}, tRNA^{LysTTT} and tRNA^{AspGTC} also tRNA^{GluCTC}. In both cases, these four types of tRNAs represent approx. 60% of all the tRNA pool in the viral particle. Other tRNAs were packed rather randomly. Surprisingly, the types of co-packed tRNAs in iflaviruses (tRNA^{LysCTT}, tRNA^{LysTTT} and tRNA^{AspGTC}) are typical tRNA co-packed also by human retrovirus HIV-1, where tRNA^{LysTTT} serves as primer for reverse transcription.^[20] The role of the other tRNAs in HIV-1 viral particle is not well understood. It was suggested that other non-complemental tRNA may contribute to retroviral replication by shielding the membrane binding surface of the HIV matrix protein domain from the interactions with intracellular membranes before the Gag protein reaches the cellular membrane.^[13d,21] Another hypothesis proposes that these tRNAs assist in HIV-1 nuclear transport^[22] or that HIV-1 changes the host tRNA pool to enrich those tRNAs encoded in A-rich HIV genome.^[23] As viruses from the order *Picornavirales* do not encode for Gag protein and their genomes are not transported into or out of nucleus, we cannot apply the retroviral explanation on them.

The main difference between packed tRNAs by retroviruses and *Picornavirales* is their size. While we detected full matured tRNAs in HIV-1,^[13a] SBV and DWV contained 3' and 5' tRNA fragments. The production of such tRNA fragments was described under stress conditions and viral infection.^[24] Particularly, it was shown that infection by respiratory syncytial virus (RSV, -ssRNA virus) leads to generation of 3' and 5' tRNA fragments.^[25] 5' tRNA fragments generated from tRNA^{GlyGCC} and tRNA^{LysCTT} promote RSV replication.^[24] While part of 5' tRNA fragment generated from tRNA^{GluCTC} recognizes 3'-UTR of anti-RSV protein – apolipoprotein E receptor 2 and suppress its expression.^[26] 3' end tRNA fragments generated from Proline tRNA were also detected in virus particles of human T-cell leukemia virus type 1, where they serve as primers for reverse transcriptase.^[27] So far, the tRNA fragments have not been detected in +ssRNA viral particles. Nevertheless, our data together with previously reported tRNA fragments in other types of viruses suggest that the role of tRNA fragments can be quite general and that they may enhance viral replication or

suppress antiviral response of host organism. The further studies will be necessary to explain this phenomenon and reveal real function of the co-packed tRNA fragments. For this purposes, model production of the insect viruses in tissue cell cultures will have to be established to allow functional experiments.

Recently, it was shown that double-stranded RNA regions from Flock House Virus genomic RNA were interacting with the capsid protein.^[28] The disruption of these structures by mutations resulted in changes in viral replication, propagation, and packaging. The presence of D and L loops of tRNA fragments may be favored by the capsid proteins of iflaviruses and thus lead to co-packing of these host RNAs. The fact that tRNA fragments and not full tRNA are co-packed can be explained by steric reasons.

In summary, we discovered that some insects iflaviruses co-pack host cellular tRNA fragments. Till now, it was believed that *Picornavirales* virions contain only viral genomic RNA. This is the first evidence, confirmed by LC-MS, RNA-seq experiments and Northern blot analysis that *Picornavirales* also pack cellular tRNA fragments. The packing of tRNA fragments is not random or dependent on intracellular concentrations of tRNAs, but it is selective and only tRNA fragments from certain types e.g. tRNA^{LysCTT}, tRNA^{LysTTT} and tRNA^{AspGTC} are present in virions. Very interesting is finding that these types of tRNAs or fragments are also co-packed by virions of retroviruses such as HIV-1 or in RSV virions.

Experimental Section

Production and purification of honeybee viruses

SBV and DWV were purified as described previously.^[12b,29] Briefly: one hundred experimentally infected honeybee pupae were homogenized using a Dounce homogenizer (piston-wall distance 0.075 mm) in 50 mL of phosphate buffered saline (PBS) on ice. The extract was centrifuged at 15,000×g for 30 min at 10 °C. The pellet was discarded, and the supernatant was ultracentrifuged at 150,000×g for 3 h in a Ti50.2 fixed-angle rotor (Beckman-Coulter) at 10 °C. The resulting pellet was resuspended in PBS in a final volume of 10 mL. MgCl₂ was added to a final concentration of 5 mM as well as 20 µg/mL of DNase I and 20 µg/mL of RNase. The solution was incubated at room temperature for 30 min and centrifuged for 15 min at 5,500 g at room temperature. The resulting supernatant was loaded onto 0.6 g/mL CsCl in PBS and centrifuged for 16 h at 30,000 rpm in an SW41 swinging-bucket rotor at 10 °C (Beckman-Coulter). Virus bands were collected by the gentle piercing of ultracentrifuge tubes with an 18-gauge needle. The viruses were buffer-exchanged to PBS and concentrated using centrifuge filter units with a 100-kDa molecular mass cutoff.

Production and purification of human viruses

Echovirus 18 (strain METCALF, obtained from ATCC-VR-852TM) was propagated in immortalized African green monkey kidney (GMK, 84113001 Sigma) cells cultivated in Dulbecco's modified Eagle's medium enriched with 10% fetal bovine serum. RV2 (strain HGP, ATCC-482) was propagated in HeLa (ATCC-CCL2) cells cultivated in Dulbecco's modified Eagle's medium enriched with 10% fetal bovine serum. For virus preparation, 50 tissue culture dishes with a

diameter of 150 mm of cells grown to 100% confluence were infected with a multiplicity of infection of 0.01. The infection was allowed to proceed for 2–3 days, at which point more than 90% of the cells exhibited a cytopathic effect. The cell media were harvested, and any remaining attached cells were removed from the dishes using cell scrapers. The cell suspension was centrifuged at 15,000×g in a Beckman Coulter Allegra 25R centrifuge, rotor A-10 at 10 °C for 30 min. The resulting pellet was resuspended in 10 mL of PBS. The solution was subjected to three rounds of freeze-thawing by transfer between –80 °C and 37 °C and homogenized using a Dounce tissue grinder. Cell debris was separated from the supernatant by centrifugation at 3,100×g in a Beckman Coulter Allegra 25R centrifuge, rotor A-10, at 10 °C for 30 min. The resulting supernatant was added to the media from the infected cells. Virus particles were precipitated by the addition of PEG-8000 and NaCl to final concentrations of 12.5% (w/v) and 0.6 M, respectively, and incubation overnight at 10 °C with mild shaking. The precipitate was centrifuged at 15,000×g in a Beckman Coulter Allegra 25R centrifuge, rotor A-10, at 10 °C for 30 min. The white precipitate was resuspended in 12 mL of PBS. MgCl₂ was added to a final concentration of 5 mM, and the sample was subjected to DNase (10 µg/mL final concentration) and RNase (10 µg/mL final concentration) treatment for 30 min at ambient temperature. Subsequently, trypsin was added to a final concentration of 0.5 µg/mL, and the mixture was incubated at 37 °C for 10 min. EDTA at pH 9.5 was added to a final concentration of 15 mM and a non-ionic detergent, NP-40™ (SigmaAldrich Inc.), was added to a final concentration of 1%. The virus particles were pelleted through a 30% (w/v) sucrose cushion in PBS by centrifugation at 210,000×g in an Optima X80 ultracentrifuge using a Beckman Coulter™Ti 50.2 rotor at 10 °C for 2 hours. The pellet was resuspended in 1.5 mL of PBS and loaded onto a 60% (w/w) CsCl solution in PBS. The CsCl gradient was established by ultracentrifugation at 160,000×g in an Optima X80 ultracentrifuge using a Beckman Coulter™SW41Ti rotor at 10 °C for 18 h. The opaque band containing the virus was extracted with a 20-gauge needle mounted on a 5 ml disposable syringe. The virus was transferred into PBS by multiple rounds of buffer exchange using a centrifugal filter device with a 100-kDa molecular weight cutoff. The final concentration of virus particles was 2 mg/mL.

Recording of cryo-electron micrographs of virus samples

Virus suspension (3.5 µL at concentration 2 mg/mL) was applied onto holey carbon grids (Quantifoil R2/1, mesh 300; Quantifoil Micro Tools) and vitrified by plunging into liquid ethane using an FEI Vitrobot Mark IV. Grids with the vitrified sample were transferred to an FEI Titan Krios electron microscope operated at 300 kV aligned for parallel illumination in nanoprobe mode. The sample in the column of the microscope was kept at –196 °C. Images were recorded with a Falcon III direct electron detection camera under low-dose conditions (46 e[–]/Å²) with under focus values about 3 µm at a nominal magnification of 75,000, resulting in a pixel size of 1.07 Å/pixel.

RNA isolation

RNA from *Iflaviruses* (SBV and DWV) and human *Picornaviruses* E18 and RV2 was isolated by Zymo-Spin™ IIC Columns (Direct-zol™ RNA MiniPrep Plus, Zymo) according to the manufacturer's protocol. RNA from honeybee was isolated from the whole body using TRIzol reagent according to the manufacturer's protocol. The quality of RNA samples was checked by HS RNA ScreenTape (4200 TapeStation, Agilent, Figure S1 8). RNA samples were quantified by an RNA High Sensitivity Assay (Qubit 4 Fluorometer, ThermoFisher).

RNA digestion and LC–MS analysis

Picornaviral RNA samples (1–10 µg) were fully digested by Nuclease P1 (1 U/µg of RNA, Sigma-Aldrich). Reaction was performed in 50 mM ammonium acetate buffer (pH 4.5) at 37 °C for 1 hour. After addition of Calf Intestine Alkaline Phosphatase (CIP, 1 U/µg of RNA, New England BioLabs) and CutSmart buffer (final concentration 1×), the samples were incubated for another 1 hour at 37 °C. Digested RNA samples were diluted in 200 µL and purified over Microcon® – 10 kDa centrifugal filters (Merck). The flow-through was concentrated using a SpeedVac system to the volume of 20 µL for LC–MS analysis.

The separation of the digested RNA was performed on an LC system (I–Class, Waters) with a C18 column (Acquity UPLC® BEH C18 1.7 µm, Waters) at 40 °C in gradient of 0.1% (v/v) formic acid in water (A) and 0.1% (v/v) formic acid in acetonitrile (B). The gradient was 0–6 min, 100% A; 6–7.5 min, 100–99% A; 7.5–9.5 min, 99–94% A; 9.5–15 min, 94% A; 15–25 min, 94–50% A; 25–27 min, 50–20%; 27–29.5 min, 20% A; 29.5–30 min, 20–100% A; 30–40 min, 100% A. The flow rate was 0.05 mL/min. The autosampler cooled the samples to 8 °C. The LC system was coupled on-line to a mass spectrometer (Synapt G2, Waters) to acquire masses of nucleosides by electrospray ionization. Ions were scanned in a positive polarity mode over full-scan range of *m/z* 100–1200. The source parameters were as follows: capillary voltage, 3 kV; source temperature, 150 °C; sampling cone, 40; extraction cone, 5; desolvation temperature, 450 °C; desolvation gas flow, 600 L/h.

LC–MS data (chromatograms) were analyzed by software MassLynx V4.1. A mixture of nucleoside standards from each canonical and methylated nucleoside (A, m¹A, m⁶A, Am; G, m¹G, m²G, m⁷G, Gm; C, m³C, m⁵C, Cm; U, m⁵U, Um) were measured in ratio 100× canonical base: 1×methylated bases. Standard mixtures were injected on a column to compare the response of each nucleoside under defined ionization conditions. The mixture was measured in the technical triplicate. For each standard, an extracted ion chromatogram (XIC) was generated using a major fragment observed in its full scan spectrum (fragmentation occurs in the ion source). The chromatographic peaks in XICs were integrated. The standard peak area (area under the curve, AUC) was used to calculate the ionization efficiency ratio of the tested nucleosides.

The chromatographic peaks of the major fragments in XICs were integrated and the AUC was used to calculate the amount of each modification per 100 unmodified nucleosides (Figure 1b).

RNA sequencing library preparation

m¹A mapping: The first RNA-seq library was prepared from SBV isolated RNA by protocol described previously.^[13a] Shortly, chemical fragmentation (metal-ion induced) was used to achieved size distribution of fragments from 50–200 nt. Samples were ethanol precipitated. To have a negative control, rearrangement of m¹A to m⁶A was performed by alkali treatment. One-half of each sample was incubated with alkaline buffer (50 mM Na₂CO₃, 2 mM EDTA, pH 10.4) for 1 h at 60 °C and purified by RNA Clean & Concentrator columns (Zymo). After adaptor ligation and couple of purification steps reverse transcriptase (RT) was used. To confirm the position of m¹A two RTs (SuperScript™ III reverse transcriptase and TGIRT™ reverse transcriptase) were used. Each should show different pattern (misincorporation or break) when meet m¹A. RNA was degraded and after cDNA tailing and barcode-labeling samples were submitted for sequencing on Ion Torrent platform.

Bisulfite sequencing: For second library (SBV, DWV) was used similar protocol but additional step of bisulfite treatment was added. After chemical fragmentation, one half of SBV and DWV

samples was used for bisulfite conversion. This was done by EZ RNA Methylation™ Kit (Zymo Res. Com.) according to the manufacturer's protocol. The quality of RNA samples was checked by HS RNA ScreenTape (4200 TapeStation, Agilent). RNA samples were quantified by an RNA High Sensitivity Assay (Qubit 4 Fluorometer, Thermofisher). Samples were purified and concentrated by ethanol precipitation and submitted for sequencing on Ion Torrent platform. Only SuperScript™ III reverse transcriptase was used to prepare this library.

Bioinformatic analysis

After quality control performed by FastQC (<https://www.bioinformatics.babraham.ac.uk/projects/fastqc>) libraries were split by fastx toolkit (http://hannonlab.cshl.edu/fastx_toolkit/index.html) and all barcodes and technical sequences were trimmed by combination of trimomatic^[30] and cutadapt^[31] software. Sequences longer than 20bp were mapped using bwa aligner v0.7.17.^[32] We mapped reads to modified SBV (GeneBank accession NC_002066.1) and DWV (NC_004830.2) viral genomes which represent particular strains used in experiments. Honeybee tRNA from the literature were clustered and only one representative for each group was used for mapping. Detection and statistical evaluation of misincorporations, insertions, deletions or premature ends were done in our own software available at <https://github.com/bioinfocfz/rnamod> under MIT license. Program uses a SAM file generated by bwa as an input and from CIGAR string field detects differences and performs paired t-test between sample and control, then creates graphical and textual output of coverage and significant positions. Parameters for significant positions used for misincorporation and premature end were: (coverage > 100 && err > 0.4) || (coverage > 100 && p-value < 0.1 && err > 0.1); for insertion or deletion simply err > 0.3.^[33]

RNA ladder preparation

DNA templates for 21, 38 and 75 nt long RNA ladder (Table SI 12) were annealed in annealing buffer (10 mM Tris, 50 mM NaCl, 1 mM EDTA pH 7.8). In vitro transcription was performed as described^[34] in a 50 µL mixture (0.2 µM of template DNA, 1 mM of each NTP (NEB), 5% dimethyl sulfoxide (DMSO, NEB), 0.12% triton X-100 (Sigma-Aldrich), 10 mM dithiothreitol (DTT), 4.8 mM MgCl₂ (Sigma-Aldrich), 1× reaction buffer for T7 RNAP (NEB) and 125 units of T7 RNAP (New England BioLabs, NEB)). The mixture was incubated for 2 h at 37 °C. The DNA template was digested by DNase I (NEB) at 37 °C for 45 min and the enzyme was heat inactivated at 75 °C for 10 min. Samples were purified using Clean and concentrator (Zymo), mixed in ratio 1:1:1 and 3 µL were loaded on the gel.

Northern blot analysis

Denaturing polyacrylamide gel (12.5%) was prepared from Rotiphorese gel (Carl Roth) in 1×TBE buffer. The polymerized gel was pre-run at 600V for 30 min in 1×TBE buffer. All RNA samples (500 ng of honeybee RNA/well, 5000 ng of SBV RNA/well, 1200 ng or 5000 ng of DWV RNA/well) were denatured for 15 min at 55 °C and loaded into the gel wells. The gel was run at 600V for 1–2 hours and then blotted onto a charged nylon membrane (Amersham Hybond-N+; GE Healthcare) by capillary transfer in 20×SSC buffer (3 M NaCl, 0.3 M trisodium citrate, pH adjusted to 7.0) overnight. The membrane was crosslinked twice on a default setting (120 mJ, 30 s) using electronic ultraviolet crosslinker (Ultralum). The cross-linked membrane was hybridized with 10 mL of Church buffer (70 mM Na₂HPO₄, 180 mM Na₂HPO₄, 7% SDS, 1% BSA, 1 mM EDTA, pH 7.2) at 45 °C for 1 h using a ProBlot hybridization oven (Labnet). Meanwhile, 2.5 µL of 100 µM tRNA probe (Table SI 12) was end-

labelled by 10 U T4 Polynucleotide Kinase (Thermofisher Scientific) and 1 µL of γ-³²P-ATP (3.3 µM, 10 µCi/µL; Hartmann analytic) in 10 µL of supplemented kinase buffer at 37 °C for 30 min. The enzyme was inactivated at 65 °C for 5 min and the probe was purified from unincorporated nucleotides using mini Quick Spin RNA columns (Roche) according to the manufacturer's instructions. The probe was added to the membrane in 10 mL of fresh Church buffer and hybridized at 45 °C, overnight. The membranes were washed twice for 10 min each with low stringency buffer (2×SSC + 0.1% SDS) and once with high stringency buffer (0.1×SSC + 0.1% SDS), all at 45 °C. The membranes were sealed in foil, incubated with phosphor imaging plate (GE healthcare) and scanned using Typhoon FLA 9500 (GE Healthcare).

Acknowledgement

The work was supported from Ministry of Education, Youth and Sports (Czech Republic), program ERC CZ (LL1603). The bioinformatics part of the work including access to computing and storage facilities was supported by the ELIXIR CZ research infrastructure project (MEYS Grant No: LM2018131). The primary data of the RNA-seq experiments are accessible at <https://www.ebi.ac.uk/ena/browser/home> under the project accession number PRJEB53666.

Conflict of Interest

The authors declare no conflict of interest.

Data Availability Statement

The data that support the findings of this study are available from the corresponding author upon reasonable request.

Keywords: human rhinovirus type 2 · human Echovirus 18 · LC-MS · Picornavirales · RNA methylation · tRNA fragments

- [1] B. Bagiński, E. Purta, P. Piątkowski, P. Boccaletto, T. K. Wirecki, M. A. Machnicka, J. M. Bujnicki, V. de Crécy-Lagard, P. A. Limbach, R. Ross, A. Kotter, M. Helm, *Nucleic Acids Res.* **2017**, *46*, D303–D307.
- [2] a) K. D. Meyer, Y. Saletore, P. Zumbo, O. Elemento, C. E. Mason, S. R. Jaffrey, *Cell* **2012**, *149*, 1635–1646; b) D. Dominissini, S. Moshitch-Moshkovitz, S. Schwartz, M. Salmon-Divon, L. Ungar, S. Osenberg, K. Cesarkas, J. Jacob-Hirsch, N. Amariglio, M. Kupiec, R. Sorek, G. Rechavi, *Nature* **2012**, *485*, 201.
- [3] K. Slama, A. Galliot, F. Weichmann, J. Hertler, R. Feederle, G. Meister, M. Helm, *Methods* **2019**, *156*, 102–109.
- [4] F. Di Serio, E. M. Torchetti, J. A. Daròs, B. Navarro, *Viruses* **2019**, *11*, 357.
- [5] a) K. Borland, J. Diesend, T. Ito-Kureha, V. Heissmeyer, C. Hammann, A. H. Buck, S. Michalakakis, S. Kellner, *Genes* **2019**, *10*, 26; b) V. F. Reichle, S. Kaiser, M. Heiss, F. Hagelskamp, K. Borland, S. Kellner, *Methods* **2019**, *156*, 91–101; c) M. Helm, Y. Motorin, *Nat. Rev. Genet.* **2017**, *18*, 275; d) M. Helm, J. D. Alfonso, *Chem. Biol.* **2014**, *21*, 174–185.
- [6] J. F. Potužnik, H. Cahová, *mBio* **2020**, *11*, e02131–02120.
- [7] H. Hao, S. Hao, H. Chen, Z. Chen, Y. Zhang, J. Wang, H. Wang, B. Zhang, J. Qiu, F. Deng, W. Guan, *Nucleic Acids Res.* **2018**, *47*, 362–374.
- [8] A. M. Fendrick, A. S. Monto, B. Nightengale, M. Sarnes, *Archives Int. Med.* **2003**, *163*, 487–494.

- [9] H. Zhang, Y. Zhao, H. Liu, H. Sun, X. Huang, Z. Yang, S. Ma, *Sci. Rep.* **2017**, *7*, 8448.
- [10] L. M. Brutscher, A. J. McMenamin, M. L. Flenniken, *PLoS Pathog.* **2016**, *12*, e1005757.
- [11] S. G. Potts, J. C. Biesmeijer, C. Kremen, P. Neumann, O. Schweiger, W. E. Kunin, *Trends Ecol. Evol.* **2010**, *25*, 345–353.
- [12] a) G. Lanzi, J. R. de Miranda, M. B. Boniotti, C. E. Cameron, A. Lavazza, L. Capucci, S. M. Camazine, C. Rossi, *J. Virol.* **2006**, *80*, 4998–5009; b) K. Skubnik, J. Novacek, T. Fuzik, A. Pridal, R. J. Paxton, P. Plevka, *Proc. Natl. Acad. Sci. USA* **2017**, *114*, 3210–3215; c) J. Dong, R. Guo, M. Huang, D. Wang, J. Huang, *J. Asia-Pacific Entomol.* **2020**, *23*, 76–81; d) M. Procházková, T. Fuzik, K. Skubnik, J. Moravcová, Z. Ubiparip, A. Pridal, P. Plevka, *Proc. Natl. Acad. Sci. USA* **2018**, *115*, 7759–7764.
- [13] a) A. Šimonová, B. Svojanovská, J. Trylčová, M. Hubálek, O. Moravčík, M. Zavřel, M. Pávková, J. Hodek, J. Weber, J. Cvačka, J. Pačes, H. Cahová, *Sci. Rep.* **2019**, *9*, 8697; b) A. Telesnitsky, S. Wolin, *Viruses* **2016**, *8*, 235; c) M. J. Eckwahl, H. Arnion, S. Kharytonchik, T. Zang, P. D. Bieniasz, A. Telesnitsky, S. L. Wolin, *RNA* **2016**, *22*, 1228–1238; d) M. J. Eckwahl, A. Telesnitsky, S. L. Wolin, *mBio* **2016**, *7*, e02025–15; e) M. J. Eckwahl, S. Sim, D. Smith, A. Telesnitsky, S. L. Wolin, *Genes Dev.* **2015**, *29*, 646–657.
- [14] S. K. Behura, M. Stanke, C. A. Desjardins, J. H. Werren, D. W. Severson, *Insect Mol. Biol.* **2010**, *19*, 49–58.
- [15] B. A. Elliott, H.-T. Ho, S. V. Ranganathan, S. Vangaveti, O. Ilkayeva, H. Abou Assi, A. K. Choi, P. F. Agris, C. L. Holley, *Nat. Commun.* **2019**, *10*, 3401.
- [16] R. Hauenschild, L. Tserovski, K. Schmid, K. Thüning, M. L. Winz, S. Sharma, K. D. Entian, L. Wacheul, D. L. Lafontaine, J. Anderson, J. Alfonzo, A. Hildebrandt, A. Jäschke, Y. Motorin, M. Helm, *Nucleic Acids Res.* **2015**, *43*, 9950–9964.
- [17] P. Boccaletto, M. A. Machnicka, E. Purta, P. Piątkowski, B. Bagiński, T. K. Wirecki, V. de Crécy-Lagard, R. Ross, P. A. Limbach, A. Kotter, M. Helm, J. M. Bujnicki, *Nucleic Acids Res.* **2017**, *46*, D303–D307.
- [18] K. D. Meyer, S. R. Jaffrey, *Nat. Rev. Mol. Cell Biol.* **2014**, *15*, 313–326.
- [19] M. Safra, A. Sas-Chen, R. Nir, R. Winkler, A. Nachshon, D. Bar-Yaacov, M. Erlacher, W. Rossmann, N. Stern-Ginossar, S. Schwartz, *Nature* **2017**, *551*, 251.
- [20] L. Kleiman, *IUBMB Life* **2002**, *53*, 107–114.
- [21] S. B. Kutluay, T. Zang, D. Blanco-Melo, C. Powell, D. Jannain, M. Errando, P. D. Bieniasz, *Cell* **2014**, *159*, 1096–1109.
- [22] L. Zaitseva, R. Myers, A. Fassati, *PLoS Biol.* **2006**, *4*, e332.
- [23] M. Pavon-Eternod, M. Wei, T. Pan, L. Kleiman, *RNA* **2010**, *16*, 267–273.
- [24] X. Yu, Y. Xie, S. Zhang, X. Song, B. Xiao, Z. Yan, *Theranostics* **2021**, *11*, 461–469.
- [25] J. Zhou, S. Liu, Y. Chen, Y. Fu, A. J. Silver, M. S. Hill, I. Lee, Y. S. Lee, X. Bao, *J. Gen. Virol.* **2017**, *98*, 1600–1610.
- [26] J. Deng, R. N. Ptashkin, Y. Chen, Z. Cheng, G. Liu, T. Phan, X. Deng, J. Zhou, I. Lee, Y. S. Lee, X. Bao, *Mol. Ther.* **2015**, *23*, 1622–1629.
- [27] K. Ruggero, A. Guffanti, A. Corradin, V. K. Sharma, G. De Bellis, G. Corti, A. Grassi, P. Zanovello, V. Bronte, V. Cimiale, D. M. D'Agostino, *J. Virol.* **2014**, *88*, 3612–3622.
- [28] Y. Zhou, A. Routh, *Nucleic Acids Res.* **2020**, *48*, e12–e12.
- [29] a) M. Prochazkova, K. Skubnik, T. Fuzik, L. Mukhamedova, A. Pridal, P. Plevka, *Curr. Opin. Virol.* **2020**, *45*, 17–24; b) S. Kalynych, A. Pridal, L. Palkova, Y. Levdansky, J. R. de Miranda, P. Plevka, *J. Virol.* **2016**, *90*, 7444–7455.
- [30] A. M. Bolger, M. Lohse, B. Usadel, *Bioinformatics* **2014**, *30*, 2114–2120.
- [31] M. Martin, *EMBnet. J.* **2011**, *17*, 3.
- [32] H. Li, R. Durbin, *Bioinformatics* **2009**, *25*, 1754–1760.
- [33] J. P. Didion, M. Martin, F. S. Collins, *PeerJ* **2017**, *5*, e3720.
- [34] F. Huang, *Nucleic Acids Res.* **2003**, *31*, e8–e8.

Manuscript received: May 17, 2022
Revised manuscript received: June 30, 2022
Accepted manuscript online: June 30, 2022
Version of record online: July 21, 2022